Compartmental Reaction-Diffusion Systems: Diffusion-Induced Synchrony and Symmetry-Breaking Patterns with Equal Diffusivities

Michael J. Ward (UBC, Vancouver)

Oxford Applied-Math/Math Bio Seminar June 2025

Joint with Merlin Pelz (UBC, PDF at UMinn, Sept. 2024). Thanks also to S. Iyaniwura (Moffatt Cancer Center) and J. Gou (UC Riverside)

Topic I: Diffusion-Induced Synchrony of Spatially Segregated Oscillators: Extending the Kuramoto Paradigm to Include Bulk Diffusion.

Topic II: Symmetry-Breaking Patterns with Equal Bulk Diffusivities: Binding-Mediated Pattern Formation.

Synchronization: Classical Modeling Approach: I

Weakly coupled oscillators: Let $\boldsymbol{x}_k \equiv (x_k, y_k)^T$ and μ_k be bifurcation parameters:

$$\dot{\boldsymbol{x}}_k = \boldsymbol{f}_k(\boldsymbol{x}_k; \mu_k) + \varepsilon \sum_{j=1}^{N} \boldsymbol{g}_{jk}(\boldsymbol{x}_k, \boldsymbol{x}_j), \quad k = 1, \ldots, N.$$

For N individual oscillators with frequencies ω_k without coupling, how do they synchronize under the perturbation?

Phase reductions: reduce to ODEs for the phases $\theta_k(t)$ of the oscillators where the coupling functions $H_{jk}(z)$ must be derived:

$$\dot{\theta}_k = \omega_k + \varepsilon \sum_{j=1}^{N} H_{jk}(\theta_k - \theta_j), \quad k = 1, \ldots, N.$$

Kuramoto-type models when $H_{jk}(z) = a_{jk} \sin(z)$:

$$\dot{\theta}_k = \omega_k + \varepsilon \sum_{j=1}^{N} a_{jk} \sin(\theta_k - \theta_j), \quad k = 1, \ldots, N.$$

Original Kuramoto model had $a_{jk} = 1/N$. The Kuramoto order parameter r, with $0 \leq r \leq 1$, measures the degree of phase synchronization:

$$r = \frac{1}{N} \left| \sum_{k=1}^{N} e^{i\theta_k} \right|.$$

Classical Modeling Approaches: II

Basic Results:

- Perfect phase coherence when $r = 1$.
- For $N \gg 1$, $\exists$ a phase transition to coherence at some $\varepsilon = \varepsilon_c$. When $\varepsilon < \varepsilon_c$ there is little phase coherence and r is small.

Synchronization studies of oscillators for Kuramoto-type models are ubiquitous starting from Kuramoto's seminal 1975 paper. (SIAM Moser prize 2022).

- Y. Kuramoto, *Lecture notes in Physics*, **39**, (1975).
- Y. Kuramoto, *Chemical Oscillations, Waves, and Turbulence*, Springer, (1984) (9520 google citations).
- Y. Kuramoto, H. Nakao, *Phil. Trans. A.*, **377**, (2019).
- S. Strogatz, *Physica D*, **143**, (2000); J. Acébron, *Rev. Mod. Phys.*, **77**, (2005).
- B. Pietras, A. Daffertshofer, *Physics Reports*, **819**, (2019), pp. 1–105.

One current research frontier (ICIAM 2023): coupled oscillators on networks.

Any other possibility? Today: oscillators coupled under a PDE diffusion field.

Extensions with Diffusion: Chemical Turbulence

(Kuramoto, Prog. Theor. Phys. 94, (1995)): *" Let the intrinsic dynamics of the individual cell activity be described by $\dot{\boldsymbol{u}}_j = \boldsymbol{F}(\boldsymbol{u}_j)$ which has a limit cycle. The cells are fixed in space sitting at $\boldsymbol{x}_j$. The system involves extra substance which mediates the cellular interaction. This substance is secreted from each cell, and can diffuse over the entire space."*

$$\dot{\boldsymbol{u}}_j = \boldsymbol{F}(\boldsymbol{u}_j) + \boldsymbol{g}\left[A(\boldsymbol{x}_j)\right], \qquad \varepsilon A_t = D\Delta A - A + \sum_{k=1}^{N} \boldsymbol{h}(\boldsymbol{u}_k)\delta(\boldsymbol{x} - \boldsymbol{x}_k).$$

Kuramoto (and later R. Viana (2016)) focus on the quasi-static limit $\varepsilon \to 0$:

$$\dot{\boldsymbol{u}}_j = \boldsymbol{F}(\boldsymbol{u}_j) + \boldsymbol{g}\left(\sum_{k=1}^{N} \sigma(|\boldsymbol{x}_j - \boldsymbol{x}_k|)h(\boldsymbol{u}_k)\right), \quad j = 1, \ldots, N.$$

A normal form near a Hopf bifurcation of a steady-state yields the coupled CGL equations, having a zoo of possible behaviors ("chemical turbulence"):

$$\dot{W}_j = W_j + K(1 + ic_1)\sum_{k=1}^{N} \sigma(|\boldsymbol{x}_j - \boldsymbol{x}_k|)(W_k - W_j) - (1 + ic_2)|W_j|^2 W_j, \quad j = 1, \ldots, N.$$

Limitations: A is singular at $\boldsymbol{x}_k$ in $\mathbb{R}^2$ or $\mathbb{R}^3$. How to choose g and h in applications?

Compartmental RD System: Overview

Our Modeling Framework: Nonlinear kinetics confined to a collection of spatially segregated small "cells". A passively diffusing scalar bulk species that can bind or unbind with the "cell" membrane provides the coupling mechanism and allows one intracellular species to be exchanged with the bulk.

- Inspired by C. Kuttler, et al. J. Math. Bio. **53**, (2006).
- K. Showalter, I. Epstein, Chaos **25**, (2015). *"Novel dynamical phenomena occur in structured media consisting of spatially distributed arrays of distinct interacting reacting zones... BZ reaction in a microemulusion etc..."*

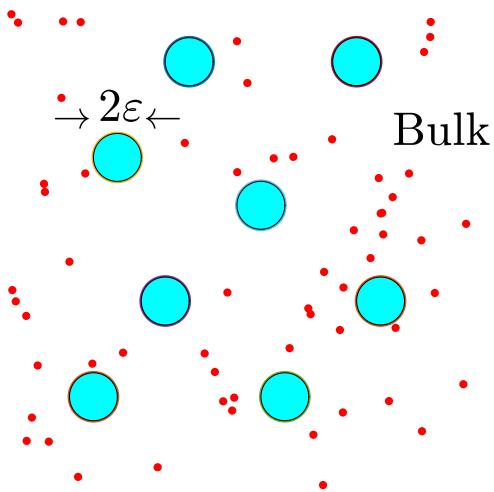

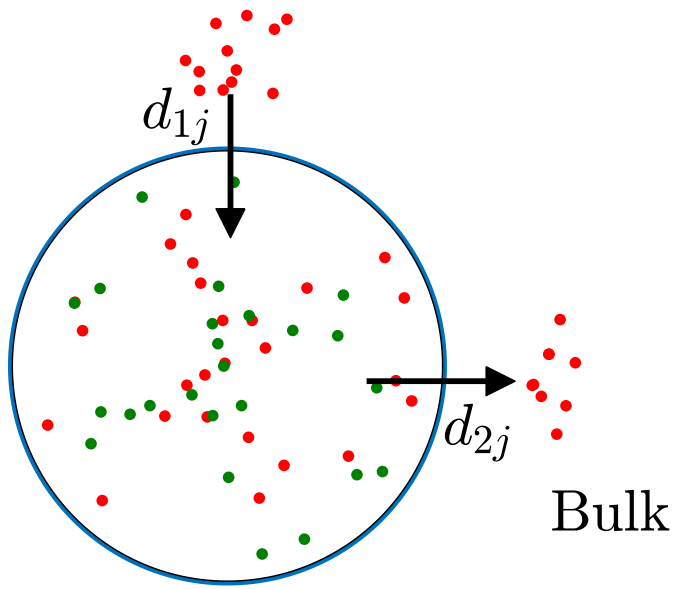

Motivation: Bulk-Cell with 1 Bulk Species

Quorum-sensing applications: involve dynamically active small "cells" that are coupled spatially by a passive scalar bulk-diffusion field (PDE) "autoinducer" (AI). Collective behavior occurs when cell population exceeds a threshold. (usually studied in the "well-mixed" limit in a finite domain from ODE's coupled to a global mode).

Collective behavior in "cells" due to coupling by diffusive chemical transport:

- Collections of unicellular (eukaryotic) organisms such as starving yeast cells (glycolysis) coupled only by extracellular signalling molecules (AI is Acetaldehyde). (**Ref:** De Monte et al., PNAS **104**(47), (2007).)
- Amoeba colonies (Dicty) in low nutrient enviroments, with cAMP organizing the aggregation of starving colonies; (**Ref:** Nanjundiah, Bio. Chem. **72**, (1998), Gregor et al. Science, **328**, (2010).)
- Catalyst bead particles (BZ particles) interacting through a chemical diffusion field; (**Ref:** Tinsley, Showalter, et al., Physica D **239** (2010).)
- Microemulsions of BZ aqueous droplets emersed in oil. (**Ref:** Tompkins et al., PNAS 2014).
- Chaotic oscillations have been observed for a compartmentalized surface reaction nanosystem. (**Ref:** Raab et al. Nature Communications 2023).

Diffusion-Mediated Communication: Two Key Features

Triggered Oscillations: emergence of intracellular oscillations from a quiescent state as either the cell density increases or reaction kinetic parameters change (i.e. glycolysis, social amoeba, catalyst bead particles).

- In the absence of coupling by bulk diffusion, the "cells" are in a quiescent state. Oscillations occur via a switchlike response (Hopf bifurcation (HB)).
- Analysis: find steady-states and identify when a HB occurs.

Synchronized Oscillations: How do intracellular oscillations that are occuring within each "cell" synchronize owing to the PDE cell-bulk coupling?

- Analysis: Must derive a new "Kuramoto-type" model for the intracellular dynamics coupled to a memory-dependent bulk diffusion field.

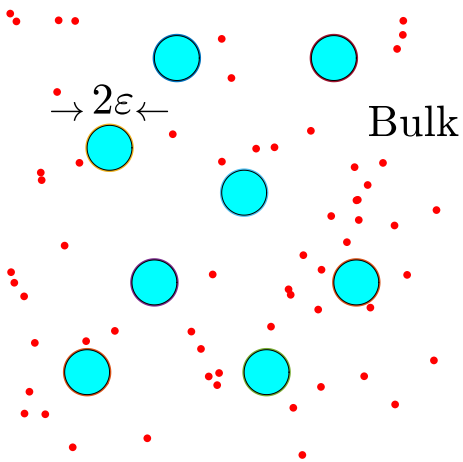

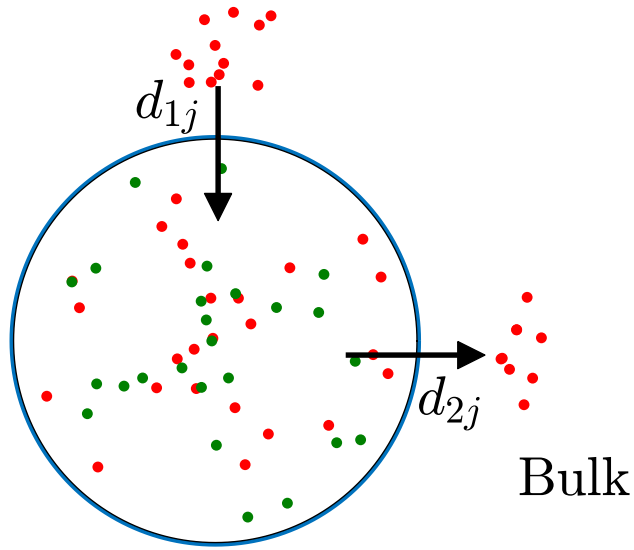

Formulation of the 2-D Model

Dimensionless Formulation: The autoinducer $U(\boldsymbol{x}, t)$ in the bulk satisfies the PDE:

$$U_t = D\Delta U - \sigma U\,, \quad \boldsymbol{x} \in \mathbb{R}^2 \backslash \cup_{j=1}^{N} \Omega_{\epsilon_j}\,; \qquad U(\boldsymbol{x}, 0) = 0\,,$$
$$\epsilon D \partial_{n_j} U = d_{1j} U - d_{2j} u_{j1}\,, \quad \boldsymbol{x} \in \partial\Omega_{\epsilon_j}\,, \quad j = 1, \ldots, N\,.$$

The cells Ω_{ϵ_j} are disks of radius $\epsilon \equiv R_0/L \ll 1$, i.e. $\Omega_{\epsilon_j} \equiv \{\boldsymbol{x}\,|\,|\boldsymbol{x} - \boldsymbol{x}_j| \le \epsilon\}$.

Inside each cell there are m interacting species $\boldsymbol{u}_j = (u_{j1}, \ldots, u_{jm})^T$, with intracellular dynamics $\boldsymbol{F}_j(\boldsymbol{u}_j)$ for each $j = 1, \ldots, N$:

$$\frac{d\boldsymbol{u}_j}{dt} = \boldsymbol{F}_j(\boldsymbol{u}_j) + \frac{\boldsymbol{e}_1}{\varepsilon} \int_{\partial\Omega_{\epsilon_j}} \left(d_{1j} U - d_{2j} u_{j1}\right)\, ds\,, \qquad \boldsymbol{e}_1 \equiv (1, 0, \ldots, 0)^T\,.$$

Note: Time-scale is wrt dimensional intracellular reaction rate k_R. Dimensionless parameters: d_{1j} (influx), d_{2j} (efflux); σ (bulk decay rate); D (effective diffusivity);

$$\sigma \equiv \frac{k_B}{k_R}\,, \qquad D \equiv \left(\frac{\sqrt{D_B/k_R}}{L}\right)^2\,, \quad L = \min|\boldsymbol{x}_i - \boldsymbol{x}_j|\,.$$

Asymptotic Limit: We will consider the singular perturbation limit $\varepsilon \to 0$.

New Reduction: Memory-Dependent Oscillations in 2-D: I

Main Result

For $\varepsilon \to 0$, and with $U(\boldsymbol{x};0) = 0$, the intracelllular dynamics $\boldsymbol{u}_j(t)$ for $j = 1, \ldots, N$ is approximated for $t \gg \mathcal{O}(\varepsilon^2)$ by the integro-differential ODE system:

$$\frac{d\boldsymbol{u}_j}{dt} = \boldsymbol{F}_j(\boldsymbol{u}_j) + \boldsymbol{e}_1 B_j(t)\,,$$

$$\int_0^t B_j{}'(\tau) E_1(\sigma(t-\tau))\,d\tau = \eta_j B_j(t) + \gamma_j u_{j1}(t) + \sum_{\substack{k=1 \\ k\neq j}}^{N} \int_0^t \frac{B_k(\tau) e^{-\sigma(t-\tau)}}{(t-\tau)} e^{-|\boldsymbol{x}_j - \boldsymbol{x}_k|^2/(4D(t-\tau))}\,d\tau\,.$$

Here $E_1(z)$ is the exponential integral, γ_e is Euler's constant, and η_j and γ_j are

$$\eta_j = -\log(\varepsilon^2 \kappa_{0j} \sigma)\,, \qquad \gamma_j \equiv \frac{4\pi D d_{2j}}{d_{1j}}\,, \quad \textit{with} \quad \kappa_{0j} \equiv \frac{e^{2(\gamma_e - D/d_{1j})}}{4D}\,.$$

Memory-Dependent Oscillations in 2-D: II

- In the bulk region at $\mathcal{O}(1)$ distances from the cell centers, we have for $\varepsilon \to 0$

$$U(\boldsymbol{x},t) \sim -\frac{1}{4\pi D}\sum_{j=1}^{N}\int_0^t \frac{B_j(\tau)e^{-\sigma(t-\tau)}}{(t-\tau)} e^{-|\boldsymbol{x}-\boldsymbol{x}_j|^2/(4D(t-\tau))}\,d\tau\,.$$

- In the vicinity of the j^{th} cell we have for $\rho = \varepsilon^{-1}|\boldsymbol{x}-\boldsymbol{x}_j| = \mathcal{O}(1)$ that

$$U \sim \frac{B_j(t)}{2\pi D}\log\rho + \frac{B_j(t)}{2\pi d_{1j}} + \frac{d_{2j}}{d_{1j}}u_{j1}(t)\,.$$

- **This is a new "Kuramoto"-type system for memory-dependent oscillations of spatially segregated oscillators coupled by bulk diffusion. Ref: M. Pelz, M. J. Ward, Synchronized Memory-Dependent Intracellular Oscillations for a Cell-Bulk ODE-PDE Model in $\mathbb{R}^2$, SIADS, 24(2), (2025) (60 pages).**
- Valid for arbitrary initial values $\boldsymbol{u}_j(0) \geq 0$. Must analyze the initial transient from the PDE to get the asymptotic matching behavior for $B_j(t)$ as $t \to 0^+$.
- Derivation: extend strong localized perturbation theory to a time-dependent setting.

2-D Transient Analysis Near a Cell

Assume $u_{j1}(0) > 0$. Near j^{th} cell let $t = \varepsilon^2\tau$. Then, $V(\rho,\tau) = U(\boldsymbol{x}_j + \varepsilon\boldsymbol{y}, \varepsilon^2\tau)$ satisfies the leading-order "inner" problem (solvable by Laplace transforms):

$$V_\tau = D\left(V_{\rho\rho} + \frac{1}{\rho}V_\rho\right), \quad \rho > 1, \ \tau \geq 0; \quad V(\rho,0) = 0,$$
$$DV_\rho = d_{1j}V - d_{2j}u_{j1}(0), \quad \text{on } \rho = 1.$$

Main Result

Suppose $u_{j1}(0) > 0$. For ρ fixed and $\tau \gg 1$, we have

$$V(\rho,\tau) \sim u_{j1}(0)\frac{d_{2j}}{d_{1j}} + \frac{B_j(\tau)}{2\pi D}\left(\log\rho + \frac{D}{d_{1j}}\right),$$
$$B_j(\tau) \sim -\frac{4\pi D d_{2j}u_{1j}(0)}{d_{1j}\log\left(\tau/\left[\kappa_{0j}e^{-\gamma_e}\right]\right)} + \mathcal{O}\left(\left[\log\left(\tau/(\kappa_{0j}e^{-\gamma_e})\right)\right]^{-2}\right).$$

With $t = \varepsilon^2\tau$, we have $|B_j'(t)| \to \infty$ as $t \to 0^+$ if $u_{j1}(0) > 0$.

Key: This far-field behavior of the transient solution is essential for providing the "initial conditions" for $B_j(t)$ for the integro-differential ODE system.

Outline of Derivation: Singular Perturbation Theory I

"Quasi-Static Slender-Body Approximation:" For $t = \mathcal{O}(1)$, in the j^{th} inner region set $V(\boldsymbol{y}, t) = U(\boldsymbol{x}_j + \varepsilon \boldsymbol{y}, t)$ and $\boldsymbol{y} = \varepsilon^{-1}(\boldsymbol{x} - \boldsymbol{x}_j)$ to get

$$\Delta_{\boldsymbol{y}} V = 0\,, \quad \text{for} \quad \rho = |\boldsymbol{y}| > 1\,; \qquad DV_\rho = d_{1j} V - d_{2j} u_{j1}(t)\,, \quad \text{on} \quad \rho = 1\,.$$

For some $B_j(t)$, the radially symmetric solution is

$$V(y,t) = \frac{B_j(t)}{2\pi D} \log|\boldsymbol{y}| + \frac{B_j(t)}{2\pi d_{1j}} + \frac{d_{2j}}{d_{1j}} u_{j1}(t)\,.$$

Self-consistent "Kuramoto model with diffusion": In terms of $B_j(t)$, we have

$$\frac{d\boldsymbol{u}_j}{dt} = \boldsymbol{F}_j(\boldsymbol{u}_j) + B_j(t)\boldsymbol{e}_1\,, \quad j = 1, \ldots, N\,,$$

where, from asymptotic matching of inner and bulk solutions, $B_j(t)$ is found from

$$U_t = D\Delta U - \sigma U\,, \quad \boldsymbol{x} \in \mathbb{R}^2 \backslash \{\boldsymbol{x}_1, \ldots, \boldsymbol{x}_N\}\,; \qquad U(\boldsymbol{x}; 0) = 0\,,$$

$$U \sim \frac{B_j}{2\pi D} \log|\boldsymbol{x} - \boldsymbol{x}_j| + \frac{B_j}{2\pi D\nu} + \frac{B_j}{2\pi d_{1j}} + \frac{d_{2j}}{d_{1j}} u_{j1}\,, \ \text{as} \ \boldsymbol{x} \to \boldsymbol{x}_j\,, \ j = 1, \ldots, N\,, \quad (1)$$

$$U(\boldsymbol{x}, t) \to 0\,, \quad \text{as} \quad |\boldsymbol{x}| \to \infty \quad \text{for} \quad t > 0\,.$$

Here $\nu \equiv -1/\log\varepsilon$.

Outline of Derivation: Singular Perturbation Theory II

Consider an auxilliary problem for $v_k(\boldsymbol{x},t)$ given by

$$\partial_t v_k = D\Delta v_k - \sigma v_k - B_k(t)\delta(\boldsymbol{x}-\boldsymbol{x}_k)\,; \quad v_k \to 0 \quad \text{as} \quad |\boldsymbol{x}| \to \infty\,; \quad v_k(\boldsymbol{x},0) = 0\,,$$

$$v_k(\boldsymbol{x},t) \sim \frac{B_k(t)}{2\pi D}\log|\boldsymbol{x}-\boldsymbol{x}_k| + R_k(t)\,, \qquad \text{as} \quad \boldsymbol{x} \to \boldsymbol{x}_k\,.$$

$R_k(t)$ is to be found in terms of $B_k(t)$. From transient analysis: $B_k(t) \to 0$ as $t \to 0^+$.

Taking the Laplace transform: $\hat{v}_k = -\hat{B}_k\hat{G}_k$ where $\hat{G}_k(\boldsymbol{x},s)$ satisfies

$$\Delta\hat{G}_k - \frac{(\sigma+s)}{D}\hat{G}_k = -\frac{1}{D}\delta(\boldsymbol{x}-\boldsymbol{x}_k)\,; \quad \hat{G}_k \to 0 \quad \text{as} \quad |\boldsymbol{x}| \to \infty\,,$$

we calculate

$$\hat{G}_k(\boldsymbol{x},s) = \frac{1}{2\pi D}K_0\left(\sqrt{\frac{s+\sigma}{D}}|\boldsymbol{x}-\boldsymbol{x}_k|\right)\,.$$

Using the inverse Laplace transform pair $\mathcal{L}^{-1}\left(K_0(a\sqrt{s})\right) = (2t)^{-1}e^{-a^2/4t}$, we get

$$v_k(\boldsymbol{x},t) = -\int_0^t B_k(\tau)G_k(\boldsymbol{x},t-\tau)\,d\tau = -\int_0^t \frac{B_k(\tau)e^{-\sigma(t-\tau)}}{4\pi D(t-\tau)}e^{-|\boldsymbol{x}-\boldsymbol{x}_k|^2/(4D(t-\tau))}\,d\tau\,.$$

Outline of Derivation: Singular Perturbation Theory III

By expanding $\hat{v}_k(\boldsymbol{x}, s)$ as $\boldsymbol{x} \to \boldsymbol{x}_k$, we identify $\hat{R}_k(s)$. From the inverse transform:

$$R_k(t) = \frac{1}{4\pi D}\mathcal{L}^{-1}\left(s\hat{B}_k(s)\left(\frac{\log(s+\sigma)}{s}\right)\right) + \frac{B_k(t)}{2\pi D}\left(\gamma_e - \log\left(2\sqrt{D}\right)\right).$$

Since $\mathcal{L}^{-1}(s^{-1}\log(s+\sigma)) = E_1(\sigma t) + \log\sigma$, we calculate

$$R_k(t) = \frac{B_k(t)}{2\pi D}\left[\gamma_e - \log\left(2\sqrt{\frac{D}{\sigma}}\right)\right] + \frac{1}{4\pi D}\int_0^t B_k'(\tau)E_1(\sigma(t-\tau))\,d\tau\,. \qquad (2)$$

Finally, since $U(\boldsymbol{x}, t) = \sum_{k=1}^N v_k(\boldsymbol{x}, t)$ we let $\boldsymbol{x} \to \boldsymbol{x}_j$ and enforce that the limiting behavior of $U(\boldsymbol{x}, t)$ agrees with that required (magenta terms in (1)):

$$R_j(t) + \sum_{\substack{k=1\\k\neq j}}^N v_k(\boldsymbol{x}_j, t) = \frac{B_j(t)}{2\pi D}\left(\frac{1}{\nu} + \frac{D}{d_{1j}}\right) + \frac{d_{2j}}{d_{1j}}u_{j1}(t)\,, \quad j = 1, \ldots, N\,.$$

With $R_j(t)$ as in (2) $\implies$ get nonlocal system for $B_j(t)$ in terms of $u_{j1}(t)$. ■

The NAS Characterizing Steady-States

Main Result

For the memory-dependent ODE system, suppose that $B_j(0) = 0$ *and that* $B_j(t) \to B_{je}$ *and* $\boldsymbol{u}_j \to \boldsymbol{u}_{je}$ *as* $t \to \infty$ *for each* $j = 1, \ldots, N$. *Then, for* $j = 1, \ldots, N$, B_{je} *and* $\boldsymbol{u}_{je}$ *satisfy the* $N(m+1)$ *dimensional nonlinear algebraic system (NAS)*

$$\boldsymbol{F}_j(\boldsymbol{u}_{je}) + \boldsymbol{e}_1 B_{je} = 0\,, \quad \eta_j B_{je} + 2\sum_{\substack{k=1\\k\neq j}}^{N} B_{ke} K_0\left(\sqrt{\frac{\sigma}{D}}|\boldsymbol{x}_j - \boldsymbol{x}_k|\right) = -\gamma_j \boldsymbol{e}_1^T \boldsymbol{u}_{je}\,.$$

Remark: This limiting NAS coincides with what can be derived using strong localized perturbation analysis from the steady-state cell-bulk ODE-PDE system.

Linear stability of steady-states: Linearize the cell-bulk model around a steady-state:

$$U = U_s(\boldsymbol{x}) + e^{\lambda t}\Phi(\boldsymbol{x})\,, \qquad \boldsymbol{u}_j = \boldsymbol{u}_{js} + e^{\lambda t}\boldsymbol{\zeta}_j\,, \qquad j = 1, \ldots, N\,.$$

Use strong localized perturbation theory to derive a singularly perturbed PDE eigenvalue problem. Solving it $\Longrightarrow$ nonlinear matrix eigenvalue problem.

Nonlinear Matrix Eigenvalue Problem: Linear Stability

Main Result

For $\varepsilon \to 0$, any discrete eigenvalue for the linearization around a steady-state, for which $\det(\lambda I - J_j) \neq 0$ for any $j = 1, \ldots, N$ where $J_j \equiv Jac(\boldsymbol{F}_j)$, satisfies

$$\det \mathcal{M}(\lambda) = 0\,, \quad \text{where} \quad \mathcal{M}(\lambda) \equiv I + \nu \mathcal{G}_\lambda + \nu\, D\, P_1 + 2\pi\nu D P_2 \mathcal{K}(\lambda)\,,$$

with $\nu = -1/\log\varepsilon$ and where P_1, P_2 and $\mathcal{K}$ are the diagonal matrices

$$P_1 \equiv diag\Big(\frac{1}{d_{11}}, \ldots, \frac{1}{d_{1N}}\Big)\,, \qquad P_2 \equiv diag\Big(\frac{d_{21}}{d_{11}}, \ldots, \frac{d_{2N}}{d_{1N}}\Big)\,,$$

$$\mathcal{K}(\lambda) \equiv diag\,(K_1, \ldots, K_N)\,, \quad \text{where} \quad K_j \equiv \boldsymbol{e}_1^T \left(\lambda I - J_j\right)^{-1} \boldsymbol{e}_1\,.$$

The matrix $\mathcal{K}(\lambda)$ depends on intracellular kinetics $\boldsymbol{F}_j$. Moreover, $\mathcal{G}_\lambda$ is the eigenvalue-dependent Green's matrix, depending on cell locations, with matrix entries

$$(\mathcal{G}_\lambda)_{ij} = (\mathcal{G}_\lambda)_{ji} \equiv K_0\left(\sqrt{\frac{\sigma+\lambda}{D}}\,|\boldsymbol{x}_j - \boldsymbol{x}_k|\right)\,, \quad i \neq j\,,$$

$$(\mathcal{G}_\lambda)_{jj} = R_{\lambda j} \equiv \log\left(2\sqrt{\frac{D}{\sigma+\lambda}}\right) - \gamma_e\,.$$

Properties of the The GCEP

For $\varepsilon \to 0$, the set of discrete eigenvalues (point spectrum) of the linearization is

$$\Lambda(\mathcal{M}) \equiv \{\lambda \,|\, \det \mathcal{M}(\lambda) = 0\}\,.$$

Main Result

For $\varepsilon \to 0$, a steady-state (SS) solution is linearly stable when $\forall\ \lambda \in \Lambda(\mathcal{M})$ we have $Re(\lambda) < 0$. Moreover, along any parameter path of non-degenerate solutions to the NAS for which J_j is non-singular, then $\lambda = 0$ is not a root of $det\mathcal{M}(\lambda) = 0$.

- If the NAS has a unique branch of solutions as a parameter is varied, then stability cannot be lost through a zero-eigenvalue crossing on this branch. Instead, seek Hopf bifurcations with $\lambda = i\lambda_I$.
- The matrix $\mathcal{M}$ is complex-symmetric but non-Hermitian when $\lambda = i\lambda_I$.
- Effective strategies for nonlinear matrix eigenvalue problems are often restriced to Hermitian case, or where $\mathcal{M}(\lambda)$ is a polynomial or rational function of λ or where λ enters as low rank. (N. Higham, V. Mehrmann; Guttel and Tisseur, Acta Numerica, 94pp. (2017)). Not our situation!

Numerics for the GCEP

The (globally coupled) nonlinear matrix eigenvalue problem (termed the GCEP) is

$$\mathcal{M}(\lambda)\boldsymbol{c} = 0\,, \qquad \Longrightarrow \qquad \mathcal{F}(\lambda) \equiv \det\left(\mathcal{M}(\lambda)\right) = 0\,,$$

with $\mathcal{M} = \mathcal{M}(\lambda;\sigma,D)$. The number of "unstable" eigenvalues $\mathcal{Z}$ of the linearization is

$$\mathcal{Z} = \{\#\lambda \mid \mathcal{F}(\lambda) = 0\,,\ \ \mathrm{Re}(\lambda) > 0\}\,.$$

- From the winding number of $\mathcal{F}(\lambda)$ over a large semi-circle in $\mathrm{Re}(\lambda) > 0$:

$$\mathcal{Z} = \mathcal{P} - \frac{1}{\pi}\left[\arg \mathcal{F}(i\lambda_I)\right]_{\Gamma_I}\,,$$

  where Γ_I denotes the positive imaginary axis traversed upwards, and $\mathcal{P}$ is the number of poles of $\mathcal{M}(\lambda)$ in $\mathrm{Re}(\lambda) > 0$. This criterion gives $\mathcal{Z}$ at each point in the $(1/\sigma, D)$ parameter space $\Longrightarrow$ "stability map" or "scatter plot",
- HB boundaries: $\lambda = i\lambda_I(D)$ and $\sigma = \sigma(D)$ can have folds in D. Need to Compute $Re\mathcal{F}(i\lambda_I) = 0$ and $Im\mathcal{F}(i\lambda_I) = 0$ using psuedo-arclength continuation.
- For special cell configurations, the matrix spectrum of $\mathcal{M}$ is known and so computing $\mathcal{Z}$ and HB points is much simpler. Otherwise challenging if $N \gg 1$.

Properties of the The GCEP: III

What is encoded by the eigenvector $\boldsymbol{c} = (c_1, \ldots, c_m)^T$ of the GCEP $\mathcal{M}(\lambda_0)\boldsymbol{c} = 0$?

For the j^{th} cell the linearization predicts:

$$D\partial_\rho U|_{\rho=1} \sim \frac{1}{2\pi}\left(B_{je} + \sum_{\lambda_0 \in \Lambda(\mathcal{M})} c_j e^{\lambda_0 t}\right), \quad j = 1, \ldots, N,$$

$$u_{j1} \sim u_{j1e} + \sum_{\lambda_0 \in \Lambda(\mathcal{M})} K_j(\lambda_0) c_j e^{\lambda_0 t}, \quad j = 1, \ldots, N,$$

where $K_j(\lambda_0) = \boldsymbol{e}_1^T \left(\lambda_0 I - J_j\right)^{-1} \boldsymbol{e}_1$.

Qualitatively:

- If $\lambda_0 \in \mathbb{C}$, then $\mathrm{Re}\,(\mathcal{K}\boldsymbol{c})$ and $\mathrm{Im}\,(\mathcal{K}\boldsymbol{c})$ encode both the relative magnitude and phase shift of small-scale oscillations for the permeable species u_{j1}.
- The relative magnitude of c_j measures the strength of the signaling gradient $D\partial_\rho U$ on the cell boundary $\rho = 1$ and so informs "diffusion-sensing".

Three Key Numerical Challenges

Challenge I: Numerical Computation of Integro-Differential System: A "naive" integration would involve discretizing $N(N+1)/2$ memory-dependent convolution integrals, each with integrable singularities, on a time interval t to advance the solution one time step to time $t + \Delta t$. Impractical! (Need a time-marching scheme).

Challenge II: Scatter plot or Stability Phase diagram: Must compute $\mathcal{Z}$ at each point in the $1/\sigma$ versus D parameter plane (pixelated) from:

$$\mathcal{Z} = \mathcal{P} - \frac{1}{\pi}\left[\arg \mathcal{F}(i\lambda_I)\right]_{\Gamma_I}, \qquad \mathcal{F}(i\lambda_I) = \det \mathcal{M}(i\lambda_I).$$

Special spatial configurations of cells: computed by finding matrix spectrum of $\mathcal{M}$.

General: since $\mathcal{M}$ is complex symmetric $\exists$ an approach using a Takagi factorization.

Challenge III: Numerical computation of HB parameter paths satisfying $\det \mathcal{M}(i\lambda_I) = 0$ for a large $N \approx 100$ of non-identical cells with no special matrix structure. (Not clear the best way to proceed.)

Challenge I: Numerics for the Integro-Differential System

Need to numerically solve the integro-differential system for $\boldsymbol{u}_j$ and B_j, $j = 1, \ldots, N$:

$$\frac{d\boldsymbol{u}_j}{dt} = \boldsymbol{F}_j(\boldsymbol{u}_j) + \boldsymbol{e}_1 B_j(t)\,,$$

$$\int_0^t B_j'(\tau) E_1(\sigma(t-\tau))\, d\tau = \eta_j B_j(t) + \gamma_j u_{j1}(t) + \sum_{\substack{k=1 \\ k\neq j}}^{N} \int_0^t \frac{B_k(\tau) e^{-\sigma(t-\tau)}}{(t-\tau)} e^{-a_{jk}^2/(t-\tau)}\, d\tau\,,$$

where $a_{jk} \equiv |\boldsymbol{x}_j - \boldsymbol{x}_k|/\sqrt{4D}$. Blue terms are the "nonlocal part".

Initial conditions: Can assign arbitrary initial values $\boldsymbol{u}_j(0) \geq 0$. Recall: For $u_{j1}(0) > 0$ the transient analysis provided:

$$B_j(t) \sim -\frac{u_{1j}(0)\gamma_j}{\log\left(t/(\kappa_j e^{-\gamma_e})\right)}\,, \quad \text{as} \quad t \to 0\,,$$

where $\kappa_j = \kappa_{0j}\varepsilon^2$. A similar result for $B_j(t)$ can be derived when $u_{j1}(0) = 0$.

Duhamel integral: Overcoming history-dependence

Key: Develop a time-marching scheme! (Leslie Greengard's 2023 ICIAM Plenary)

Recall first a simple preliminary ODE result:

Lemma

Let $f(t)$ be continuous and define the convolution $\mathcal{F}(t) \equiv \int_0^t e^{\omega(t-\tau)} f(\tau)\, d\tau$ so that $\mathcal{F}'(t) = \omega \mathcal{F}(t) + f(t)$ with $\mathcal{F}(0) = 0$. We have the marching scheme

$$\mathcal{F}(t+\Delta t) = \mathcal{F}(t) e^{\omega \Delta t} + \mathcal{U}(t, \Delta t)\,, \quad \text{with} \quad \mathcal{U}(t, \Delta t) \equiv e^{\omega \Delta t} \int_0^{\Delta t} e^{-\omega z} f(t+z)\, dz\,.$$

An exponential time differencing ETD2 scheme, exact when $f(t)$ is linear, yields, with an error $\mathcal{O}\left((\Delta t)^3\right)$, the approximation

$$\mathcal{F}(t+\Delta t) \approx \mathcal{F}(t) e^{\omega \Delta t} + f(t) \left(\frac{e^{\omega \Delta t} - 1}{\omega} \right) + [f(t+\Delta t) - f(t)] \left(\frac{e^{\omega \Delta t} - 1 - \omega \Delta t}{\omega^2 \Delta t} \right)\,.$$

Overview: Time-Marching Scheme

Idea: Develop a marching scheme for nonlocal part of the integro-differential system

$$D_j(t) = \eta_j B_j(t) + \gamma_j u_{j1}(t) + \sum_{\substack{k=1 \\ k\neq j}}^{N} C_{jk}(t)\,,$$

$$C_{jk}(t) \equiv \int_0^t B_j(\tau) G(a_{jk}, t-\tau)\, d\tau\,, \quad G(a_{jk}, t) \equiv \frac{e^{-\sigma(t-\tau)}}{t-\tau} e^{-|\boldsymbol{x}_j - \boldsymbol{x}_k|^2/(4D(t-\tau))}\,,$$

$$D_j(t) \equiv \int_0^t B_j'(\tau)\, E_1\left(\sigma(t-\tau)\right)\, d\tau\,.$$

- Use "sum of exponentials method" applied to approximating $E_1(\sigma t)$ and $G(a_{jk}, t)$ by discretizing along certain hyperbolic-shaped paths in the Laplace parameter space. [**Refs:** Monzon and Beylkin, Appl. Comput. Harm. Anal. **28**, (2010); S. Jiang. L. Greengard, S. Wang, Adv. Comput. Math., **41**, (2015)].
- Each convolution integral has an integrable singularity at $t = \tau$. Decompose into a local part, which is approximated analytically, and a history part. For the history part, we have a Duhamel-type integral for each term in the discretization that we can update with ETD2 for a marching scheme.
- Develop a time-marching scheme for $B_j(t)$ by a ETD2 scheme applied to all the Duhamel-type integrals. Couple to the intracellular dynamics with RK4. Initial values for $B_j(t)$ known from far-field behavior of transient analysis.

Sum-of-Exponentials Approximation I

Highlight marching scheme for $D_j(t)$. Can do likewise for $C_{jk}(t)$.

The "sum-of-exponentials" approximation along a family of hyperbolic paths Γ in the Laplace transform space after path deformation from Bromwich contour Γ_B:

$$E_1(\sigma t) = \frac{1}{2\pi i} \int_\Gamma \frac{\log(1 + s/\sigma)}{s} e^{st}\, ds\,.$$

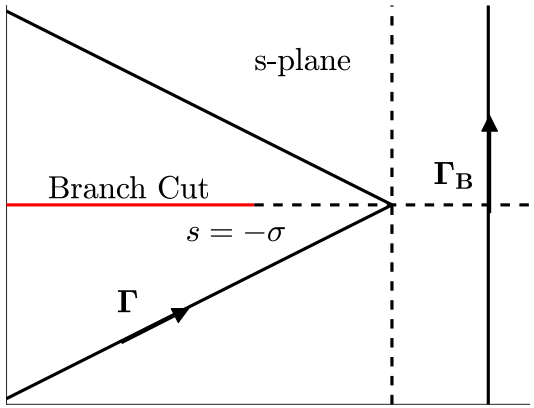

The paths are

$$\Gamma \equiv \{\, s = \chi P(x)\,,\ x \in \mathbb{R}\,\}\,, \quad \text{where} \quad P(x) \equiv 1 - \sin(\alpha + i\,x)\,.$$

By discretizing uniformly in x as $x_\ell = \ell h$, with $-n < \ell < n$, (but non-uniformly in s):

$$E_1(\sigma t) \approx E_n(t) \equiv \sum_{\ell=-n}^{n} e_\ell\, e^{s_\ell t}\,; \qquad e_\ell \equiv \frac{\chi h}{2\pi} \cos(\alpha + i\,\ell h)\, \frac{\log(1 + s_\ell/\sigma)}{s_\ell}\,, \quad s_\ell \equiv \chi P(x_\ell)\,.$$

Sum-of-exponentials approximation II

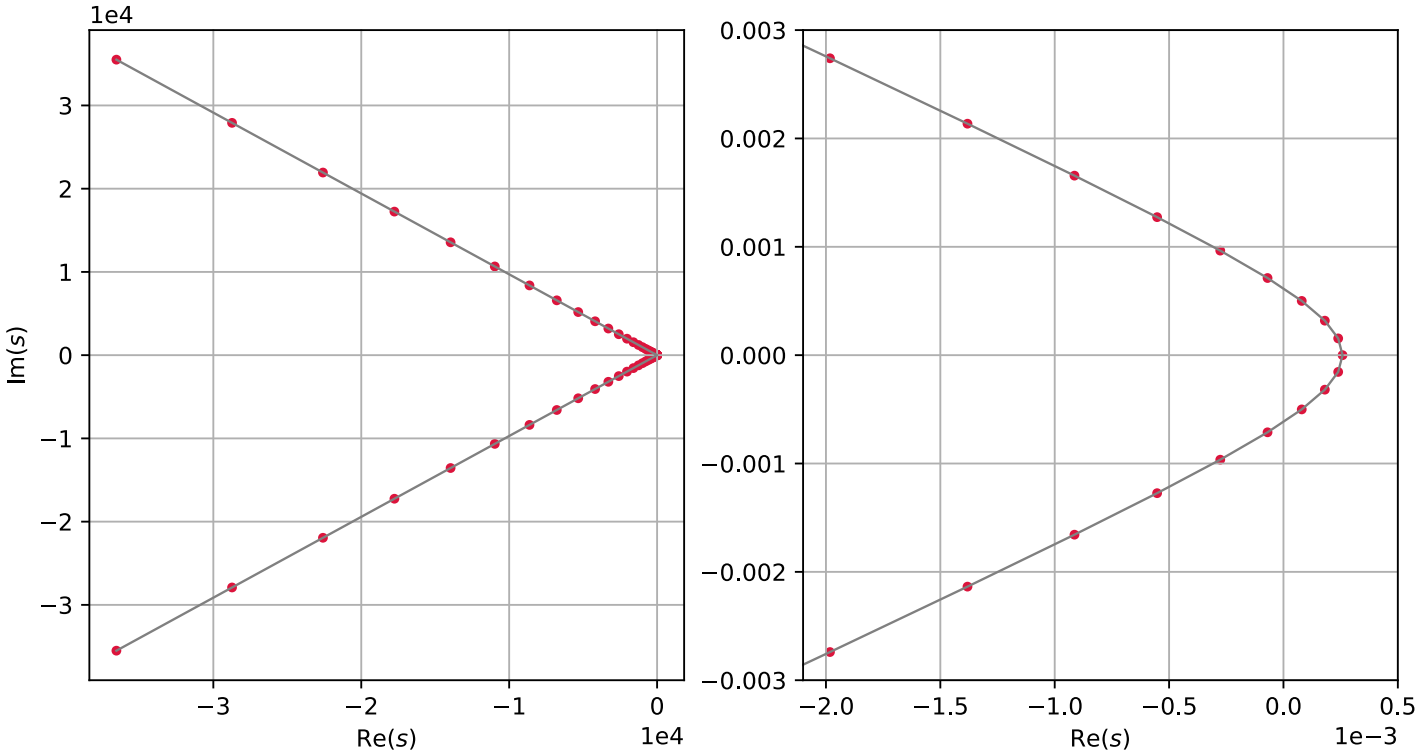

Sum-of-Exponentials Approximation III

A lemma adapted from Monzon and Beylkin (2010) gives the error in the method.

Lemma

Consider the time interval $0 < \delta \leq t \leq T_f$, *with* $T_f \geq 1000\delta$ *and let* ϵ_f *with* $0 < \epsilon_f < 0.1$ *be a prescribed error-tolerance. Then, with* h *and* χ *defined by*

$$h = \frac{a(\theta)}{n}, \quad \chi = \frac{2\pi\beta n(1-\theta)}{T_f a(\theta)}, \quad \text{where} \quad a(\theta) \equiv \cosh^{-1}\left(\frac{2T_f}{\delta(1-\theta)\sin\alpha}\right),$$

where $0 < \alpha - \beta < \alpha + \beta < \pi/2$ *and* $0 < \theta < 1$, *we have the uniform estimate*

$$|E_1(\sigma t) - E_n(t)| \leq \frac{\epsilon_f}{\sqrt{t}} \quad \text{on} \quad \delta \leq t \leq T_f,$$

when n *is sufficiently large of the order*

$$n = \mathcal{O}\left((-\log\epsilon_f + \log\log\left(T_f/\delta\right))\log\left(T_f/\delta\right)\right).$$

Optimize α, β and θ to minimize the number of terms to get a prescribed accuracy.

Key: *n* grows very slowly as either ϵ_f decreases or as T_f/δ increases.

Sum-of-exponentials approximation

Example

This sum creation for both the 2-D heat kernel and the exponential integral takes less than $2s$ for $n(I_3) = 114$.

ε_f	$n(I_1)$	$n(I_2)$	$n(I_3)$
10^{-3}	31 $(8.085 \cdot 10^{-4})$	49 $(8.663 \cdot 10^{-4})$	91 $(8.089 \cdot 10^{-5})$
10^{-6}	45 $(6.690 \cdot 10^{-7})$	75 $(9.272 \cdot 10^{-7})$	114 $(9.799 \cdot 10^{-7})$
10^{-9}	64 $(7.028 \cdot 10^{-10})$	110 $(8.417 \cdot 10^{-11})$	150 $(9.343 \cdot 10^{-10})$

Table: Number of terms $2n+1$ needed to approximate either the 2-D heat kernel with degradation $G_2(a,t) = \frac{1}{4\pi t} e^{-a^2/(4t)-\sigma t}$ with Laplace transform $\mathcal{L}[G_2](a,s) = \frac{1}{2\pi} K_0(a\sqrt{s+\sigma})$ or $E_1(\sigma t)$ to a precision ε_f for the different intervals $I_1 = [10^{-3}, 1]$, $I_2 = [10^{-3}, 10^3]$, and $I_3 = [10^{-5}, 10^4]$.

Time-Marching Scheme IV

Let $\Delta t \ll 1$. Since the kernel has an integrable singularity we decompose

$$D_j(t) = D_{Hj}(t) + D_{Lj}(t)\,, \quad \text{where} \quad D_{Hj}(t) \equiv \int_0^{t-\Delta t} B_j'(\tau) E_1\left[\sigma(t-\tau)\right]\, d\tau\,,$$

$$D_{Lj}(t) \equiv \int_{t-\Delta t}^{t} B_j'(\tau) E_1\left[\sigma(t-\tau)\right]\, d\tau = \int_0^{\Delta t} B_j'(t-z) E_1(\sigma z)\, dz\,.$$

- Local term $D_{Lj}(t)$: $D_{Lj}(t) = b_1 B_j'(t) + b_2 B_j'(t-\Delta t) + \mathcal{O}\left((\Delta t)^2\right)$.
- History term $D_{Hj}(t)$: use the sum-of-exponentials approximation:

$$D_{Hj}(t) \approx \sum_{\ell=-n}^{n} e_\ell H_{Dj\ell}(t)\,, \qquad H_{Dj\ell}(t) \equiv \int_0^{t-\Delta t} B_j'(\tau) e^{s_\ell (t-\tau)}\, d\tau\,.$$

Each history "mode" $H_{Dj\ell}(t)$ is a Duhamel integral that can be updated:

$$H_{Dj\ell}(t+\Delta t) = H_{Dj\ell}(t) e^{s_\ell \Delta t} + U_{Dj\ell}(t, \Delta t)\,,$$

$$U_{Dj\ell}(t, \Delta t) \equiv e^{2 s_\ell \Delta t} \int_0^{\Delta t} e^{-s_\ell z} B_j'(t - \Delta t + z)\, dz \approx b_{3\ell} B_j'(t) + b_{4\ell} B_j'(t-\Delta t)\,.$$

This ETD2 scheme has made the update $U_{D\ell j}$ exact for linear functions.

Overall: We can update $D_j(t+\Delta t)$ using only "local-in-time" information.

Summary: Time-Marching Scheme I:

Notation: Let $t_i = i\Delta t$ and use $B_j'(t_i) \approx \left(B_j(t_i) - B_j(t_{i-1})\right)/\Delta t$ for $i \geq 2$. Transient analysis gives $B_j'(\Delta t)$. Lag B_j in discretization. We have $B_j^{(i)} \approx B_j(i\Delta t)$, $\boldsymbol{u}_1^{(i)} \approx \boldsymbol{u}_1(i\Delta t)$, and $\boldsymbol{u}_2^{(i)} \approx \boldsymbol{u}_2(i\Delta t)$.

Step 1: $0 \curvearrowright \Delta t$: Use classical RK4 for reaction-kinetics

$$\boldsymbol{u}_1^{(1)} = \boldsymbol{u}_1^{(0)} + \frac{\Delta t}{6}(k_1^{(0)} + 2k_2^{(0)} + 2k_3^{(0)} + k_4^{(0)}) + \boldsymbol{B}^{(0)}\Delta t\,,$$
$$\boldsymbol{u}_2^{(1)} = \boldsymbol{u}_2^{(0)} + \frac{\Delta t}{6}(\tilde{k}_1^{(0)} + 2\tilde{k}_2^{(0)} + 2\tilde{k}_3^{(0)} + \tilde{k}_4^{(0)})\,,$$

with the classical RK4 weights. Here $\boldsymbol{B}^{(0)} \equiv (B_1^{(0)}, \ldots, B_N^{(0)}) = 0$.

In terms of the computed $\boldsymbol{u}_1^{(1)} \approx \boldsymbol{u}_1(t_1)$, we calculate from transient analysis $\boldsymbol{B}^{(1)} = (B_1^{(1)}, \ldots, B_N^{(1)})^T$ (and with a improved approximation):

$$B_j^{(1)} = -\frac{u_{1j}^{(1)}\gamma_j}{\log\left(\Delta t/(\kappa_j e^{-\gamma_e})\right)}\left(1 - \frac{\pi^2}{6\left[\log\left(\Delta t/(\kappa_j e^{-\gamma_e})\right)\right]^2}\right).$$

Summary: Time-Marching Scheme II:

Step 2: $\Delta t \curvearrowright 2\Delta t$: Use RK4 scheme with a lagged $\boldsymbol{B}^{(1)}$:

$$\boldsymbol{u}_1^{(2)} = \boldsymbol{u}_1^{(1)} + \frac{\Delta t}{6}(k_1^{(1)} + 2k_2^{(1)} + 2k_3^{(1)} + k_4^{(1)}) + \boldsymbol{B}^{(1)}\Delta t,$$
$$\boldsymbol{u}_2^{(2)} = \boldsymbol{u}_2^{(1)} + \frac{\Delta t}{6}(\tilde{k}_1^{(1)} + 2\tilde{k}_2^{(1)} + 2\tilde{k}_3^{(1)} + \tilde{k}_4^{(1)})\,.$$

Update $\boldsymbol{B}^{(2)}$ with

$$\boldsymbol{B}^{(2)} = A^{-1}\left(M_1 B^{(1)} + \Delta t \Gamma u_1^{(2)} - b_2 \Delta t \boldsymbol{B}'(\Delta t)\right)\,,$$

where $\boldsymbol{B}'(\Delta t)$ is given by transient solution. Here $\Gamma \equiv \mathrm{diag}(\gamma_1, \ldots, \gamma_N)$, while

$$A_{jj} = b_1 - \eta_j \Delta t\,, \qquad A_{jk} = -\Delta t E_1\left(a_{jk}^2/\Delta t\right)\,,$$
$$M_{1,jj} = b_1 - \Delta t\left(\textstyle\sum_{\ell=-n}^{n} e_\ell e^{2s_\ell \Delta t}\right)\,, \qquad M_{1,jk} = \Delta t \textstyle\sum_{\ell=-n}^{n} \omega_{jk\ell} b_{40\ell}\,,$$

for $k \neq j \in \{1, ..., N\}$. Note: $\omega_{jk\ell}$ are weights from SOE approximation for $C_{jk}(t)$.

Summary: Time-Marching Scheme III:

Step 3: Recursive-step: $t_i \curvearrowright t_{i+1}$ for $i \geq 2$:

$$\boldsymbol{u}_1^{(i+1)} = \boldsymbol{u}_1^{(i)} + \frac{\Delta t}{6}(k_1^{(i)} + 2k_2^{(i)} + 2k_3^{(i)} + k_4^{(i)}) + \boldsymbol{B}^{(i)}\Delta t\,,$$
$$\boldsymbol{u}_2^{(i+1)} = \boldsymbol{u}_2^{(i)} + \frac{\Delta t}{6}(\tilde{k}_1^{(i)} + 2\tilde{k}_2^{(i)} + 2\tilde{k}_3^{(i)} + \tilde{k}_4^{(i)})\,.$$

In terms of the computed $\boldsymbol{u}_1^{(i+1)}$ we calculate $\boldsymbol{B}^{(i+1)}$ as

$$\boldsymbol{B}^{(i+1)} = A^{-1}\left(M\boldsymbol{B}^{(i)} + \mathcal{N}\boldsymbol{B}^{(i-1)} + \left(\sum_{\ell=-n}^{n} e_\ell b_{4\ell}\right)\boldsymbol{B}^{(i-2)} + \Delta t\Gamma\boldsymbol{u}_1^{(i+1)} - \Delta t\boldsymbol{H}^{(i)}\right)\,,$$

where the matrices M and $\mathcal{N}$ have entries

$$\begin{array}{lllllll} M_{jj} & = & b_1 - b_2 - \sum_{\ell=-n}^{n} e_\ell b_{3\ell}\,, & & M_{jk} & = & \Delta t \sum_{\ell=-n}^{n} \omega_{jk\ell} b_{3\ell}\,, \\ \mathcal{N}_{jj} & = & b_2 + \sum_{\ell=-n}^{n} e_\ell (b_{3\ell} - b_{4\ell})\,, & & \mathcal{N}_{jk} & = & \Delta t \sum_{\ell=-n}^{n} \omega_{jk\ell} b_{4\ell}, \end{array}$$

for $k \neq j \in \{1, ..., N\}$.

Summary: Time-Marching Scheme IV:

The history vector $\boldsymbol{H}^{(i)} \equiv (H_1^{(i)}, \ldots, H_N^{(i)})^T$ has entries

$$H_j^{(i)} = \sum_{\ell=-n}^{n} \left(e_\ell e^{s_\ell \Delta t} H_{Dj\ell}^{(i)} - \sum_{k=1, k\neq j}^{N} \omega_{jk\ell} e^{s_\ell \Delta t} H_{Ck\ell}^{(i)} \right) ,$$

and is updated with the scheme

$$\boldsymbol{H}_{D\ell}^{(i)} = \boldsymbol{H}_{D\ell}^{(i-1)} e^{s_\ell \Delta t} + b_{3\ell} \frac{\left(\boldsymbol{B}^{(i-1)} - \boldsymbol{B}^{(i-2)}\right)}{\Delta t} + \begin{cases} b_{4\ell} \frac{\left(\boldsymbol{B}^{(i-2)} - \boldsymbol{B}^{(i-3)}\right)}{\Delta t} , & \text{if } i \geq 4 , \\ \boldsymbol{B}'(\Delta t) b_{4\ell} & \text{if } i = 3 , \end{cases}$$

$$\boldsymbol{H}_{D\ell}^{(2)} = e^{2 s_\ell \Delta t} \boldsymbol{B}(\Delta t) ,$$

$$\boldsymbol{H}_{C\ell}^{(i)} = \boldsymbol{H}_{C\ell}^{(i-1)} e^{s_\ell \Delta t} + b_{3\ell} \boldsymbol{B}^{(i-1)} + b_{4\ell} \boldsymbol{B}^{(i-2)} , \quad \text{if} \quad i \geq 3 ,$$

$$\boldsymbol{H}_{C\ell}^{(2)} = b_{40\ell} \boldsymbol{B}(\Delta t) .$$

Overall formulation: operator-splitting scheme of a semi-implicit kind. Reaction kinetics treated explicitly using RK4 with a lagged $\boldsymbol{B}^{(i-1)}$, while $\boldsymbol{u}_1^{(i)}$ appears implicitly in the update to $\boldsymbol{B}^{(i)}$. We use 114 discretization points and typically $\Delta t = 0.005$.

Examples of the Theory: Sel'kov Kinetics

Let $\boldsymbol{u} = (u_1, u_2)^T$ be intracellular dynamics given by Sel'kov kinetics:

$$F_{1j}(u_1, u_2) = \alpha_j u_2 + u_2 u_1^2 - u_1 \,, \quad F_{2j}(u_1, u_2) = \zeta_j \left(\mu_j - (\alpha_j u_2 + u_2 u_1^2)\right) \,.$$

No-bulk feedback if $d_{1j} = 0$. When isolated $d_{2j} = 0$. With boundary efflux $d_{2j} > 0$:

$$\frac{d\boldsymbol{u}_j}{dt} = \boldsymbol{F}_j(\boldsymbol{u}_j) - 2\pi d_{2j} u_{1j} \boldsymbol{e}_1 \,, \qquad \boldsymbol{e}_1 \equiv (1,0)^T \,. \tag{3}$$

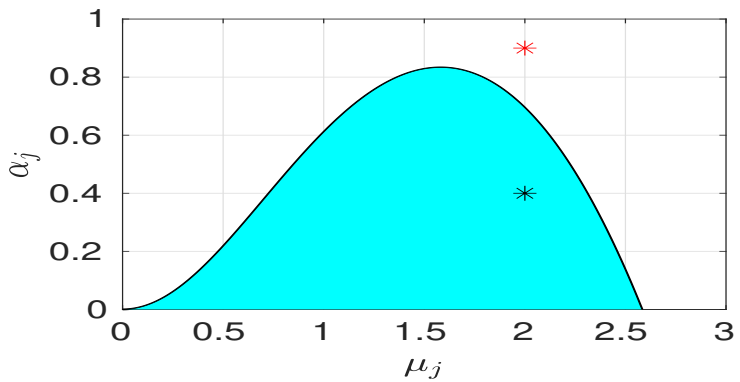

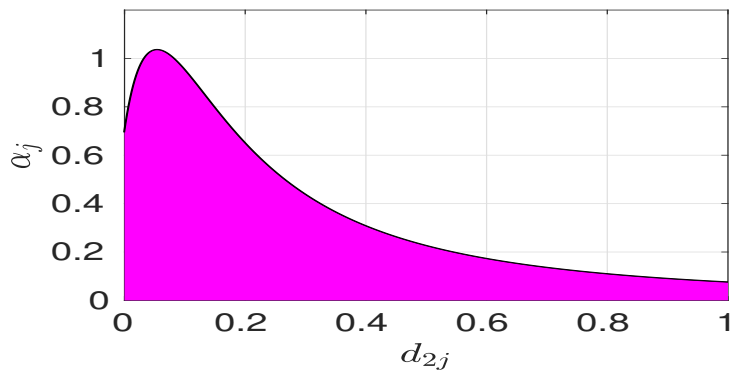

Left: limit cycle oscillations in cyan region for an isolated cell for $\zeta_j = 0.15$, $d_{1j} = d_{2j} = 0$. Right: magenta region where oscillations occur with boundary efflux d_{2j} and $\mu_j = 2$, $\zeta_j = 0.15$, $d_{1j} = 0$. For $d_{2j} \geq 0$, $\exists$ a unique SS of (3) with $\det(J_j) > 0$.

Remark: With Sel'kov kinetics, $\exists$ a unique steady-state for the cell-bulk model.

Hence, instabilities can only occur via Hopf Bifurcations.

Two-Cell Patterns and Bench-marking

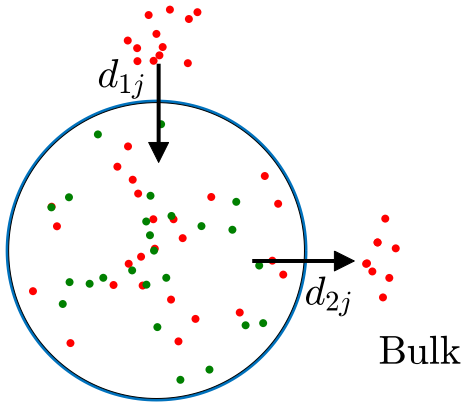

- Goal: For cell-bulk model, explore effect of changing d_{1j} (influx), d_{2j} (efflux), and kinetic parameter α_j while fixing $\varepsilon = 0.03$, $\mu_j = 2.0$, $\zeta_j = 0.15$. Allow various cell configurations.
- Typically initial conditions are chosen near the steady-state so that scatter plots can inform dynamics (at least locally).

Fast algorithm: Requires less than a minute to complete on $0 < t < 1500$ on a Dell Precision laptop i7 Intel Core with $\Delta t = 0.005$ and two cells. Algorithm run times scale well with N. Less than 3 minutes with $N = 19$.

FlexPDE commerical solver: requires many hours of CPU time with $\varepsilon = 0.03$ (cell radius) for $0 < t < 1500$ even for two cells!

$\mathbf{x}_2 = (-1, 0)$ $\mathbf{x}_1 = (1, 0)$

Two-Cell Patterns: Identical Cells I

Scatter plot in the $1/\sigma$ vs. D plane: Vary influx d_{1j} for two identical cells.

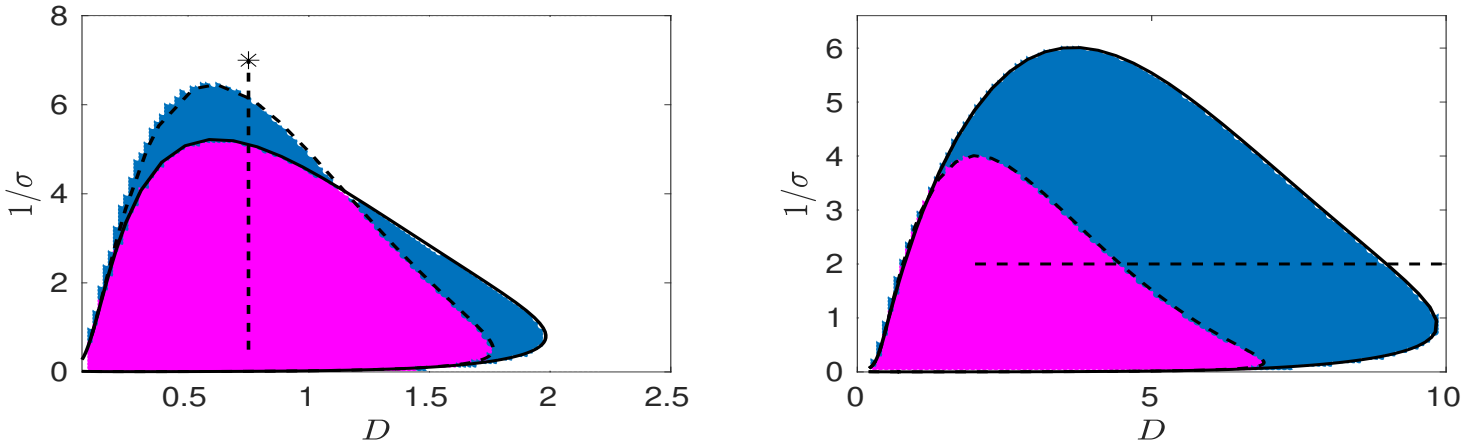

(a) $d_{1j} = 0.4$ (b) $d_{1j} = 1.5$

Figure: Two identical cells $d_{2j} = 0.2$ (efflux) and $\alpha_j = 0.9$. Cells are in a quiescent state with no cell-bulk coupling. $\mathcal{Z} = 0$ is white, $\mathcal{Z} = 2$ is blue, and $\mathcal{Z} = 4$ is magenta. The HB boundaries are superimposed: dashed HB curve is anti-phase mode $\boldsymbol{c} = (1, -1)^T$ and solid HB curve is in-phase mode $\boldsymbol{c} = (1, 1)^T$.

- $d_{1j} = 0.4$: $\exists$ a region where only anti-phase mode is unstable (top left blue).
- $d_{1j} = 1.5$: region where only in-phase mode is unstable is now much larger.

Two-Cell Patterns: Identical Cells II

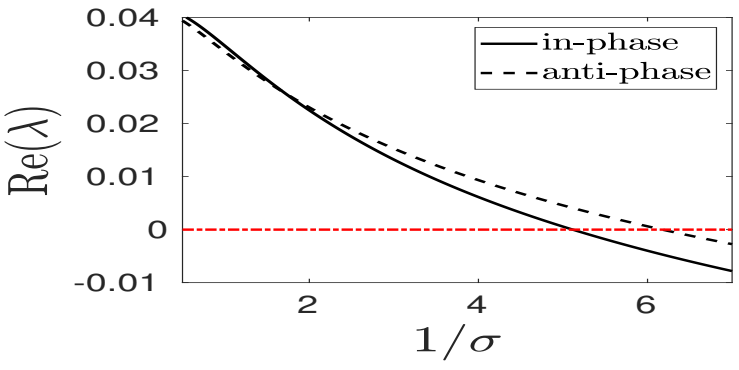

(a) Re(λ) **vertical path**

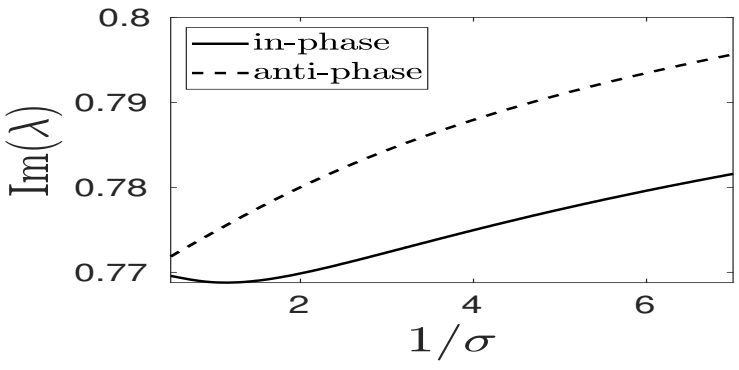

(b) Im(λ) **vertical path**

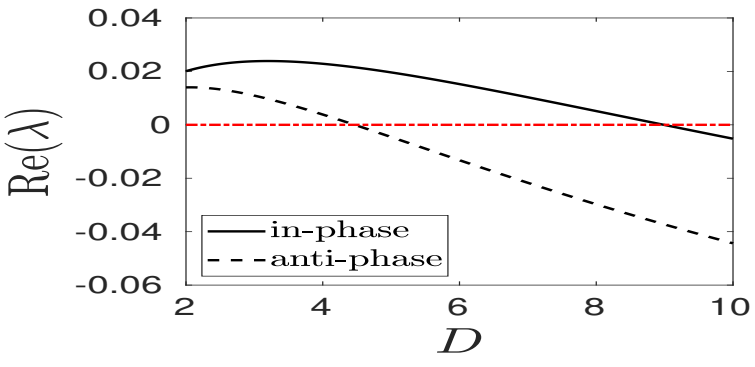

(c) Re(λ) **horizontal path**

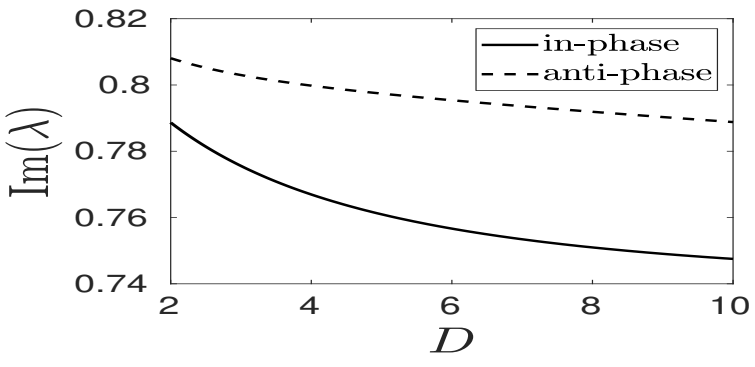

(d) Im(λ) **horizontal path**

Figure: Top row: **vertical path** with $D = 0.75$. For $\sigma = 1/7$ anti-phase mode dominates. Bottom row: **horizontal path** with $\sigma = 0.5$. In-phase mode dominates. The horizontal red line is Re$\lambda = 0$. HB frequencies do not vary much (right panels).

Two-Cell Patterns: Identical Cells III

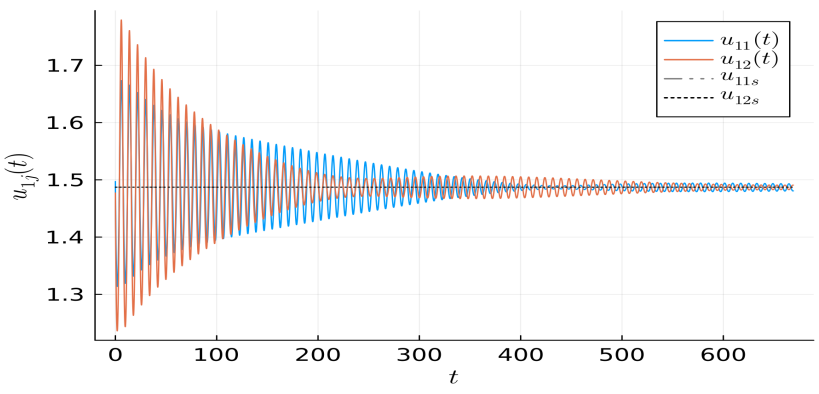

(a) u_{1j} fast algorithm

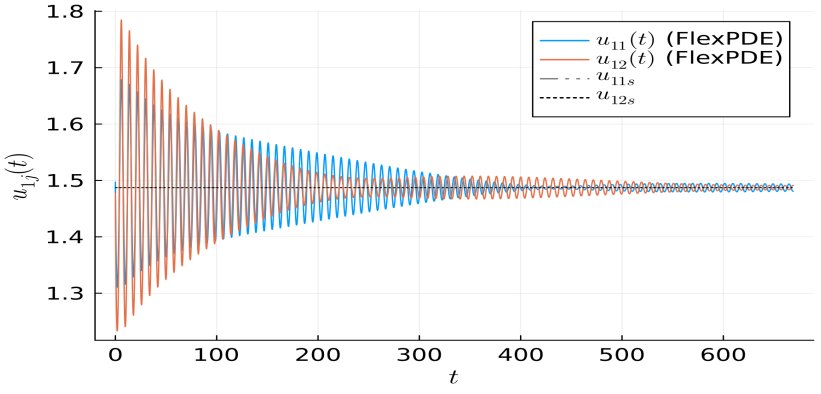

(b) u_{1j} FlexPDE

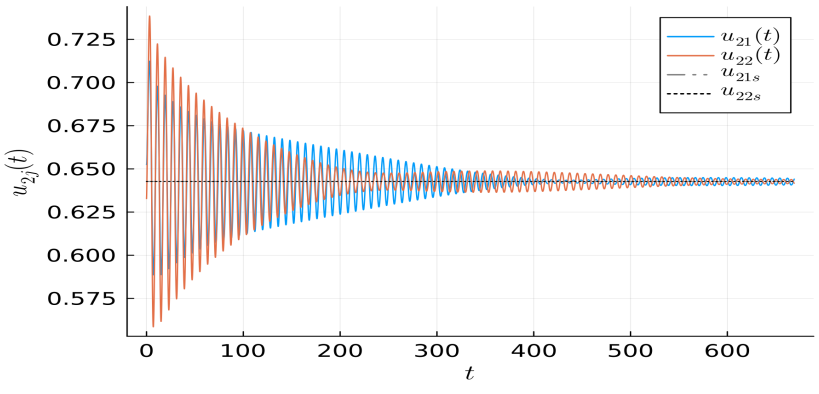

(c) u_{2j} fast algorithm

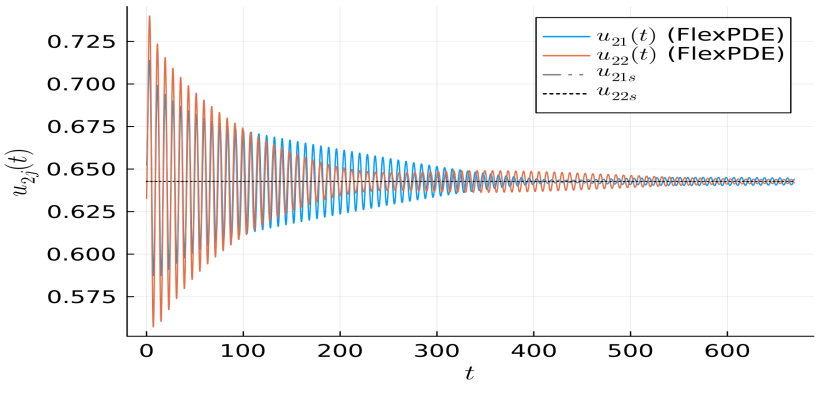

(d) u_{2j} FlexPDE

Figure: Parameters: Vertical path: $D = 0.75$, $\sigma = 1/7$ with $d_{1j} = 0.4$, $d_{2j} = 0.2$ and $\alpha_j = 0.9$. The IC imposed was the steady-state with an anti-phase perturbation: $\boldsymbol{u}_1^{(0)} = (u_{11s}, u_{21s})^T + 0.01 \cdot (1, -1)^T$, and similarly for $\boldsymbol{u}_2^{(0)}$. Also $U(\boldsymbol{x}, 0) = 0$.

Two-Cell Patterns: One Activated Cell I

Two non-identical cells: $\alpha_1 = 0.4$ and $\alpha_2 = 0.9$, with $d_{1j} = 1.5$ and $d_{2j} = 0.2$ for $j = 1, 2$. Cell with $\alpha_1 = 0.4$ is "activated": has limit cycle oscillations if uncoupled from bulk. The components of eigenvector $\boldsymbol{c}$ of $\mathcal{M}$ determine which cell is "quiet".

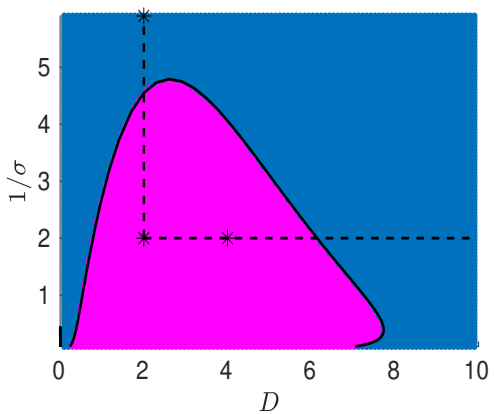

(a) Scatter plot

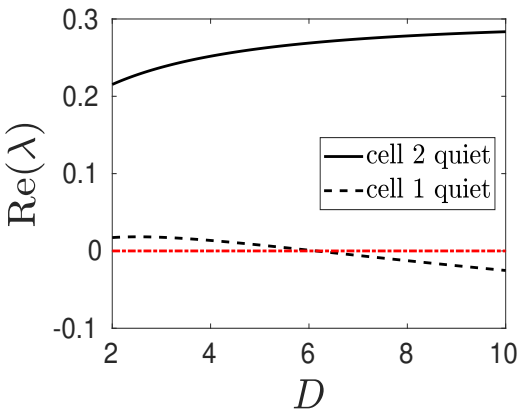

(b) Re(λ) **horizontal**

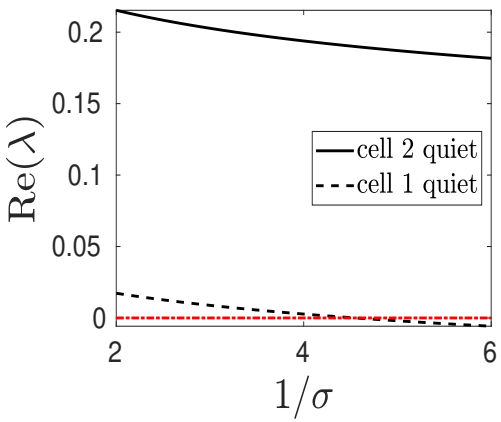

(c) Re(λ) **vertical**

Key: As expected, the dominant mode of instability is for intracellular oscillations to be concentrated to the first cell, while the second cell is essentially quiescent.

Two-Cell Patterns: One Activated Cell II

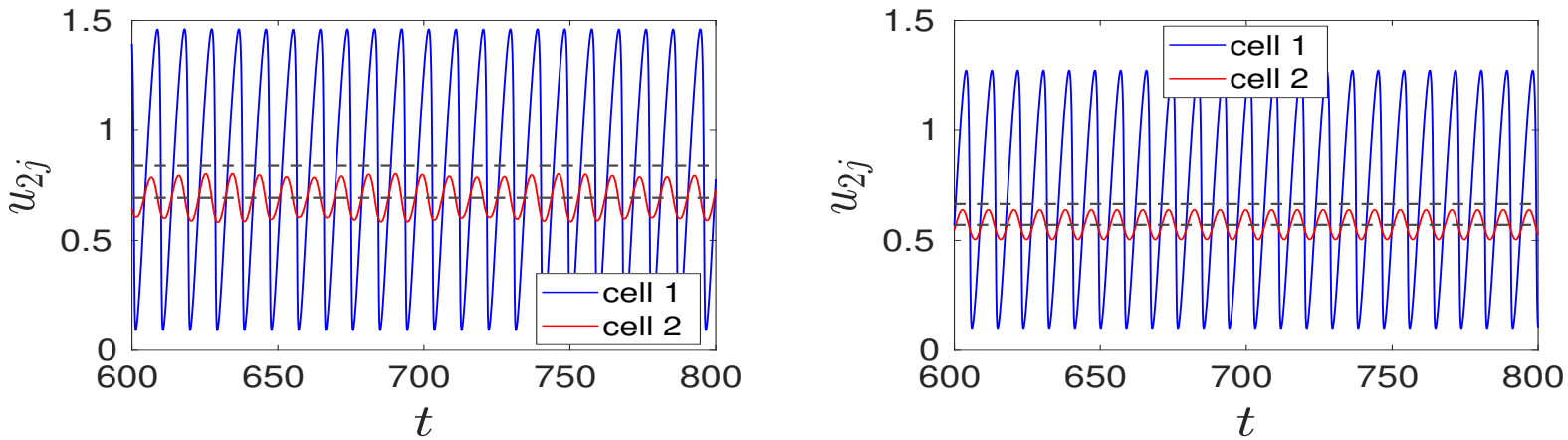

(a) $D = 4$, $\sigma = 1/2$. (b) $D = 2$, $\sigma = 1/6$.

Figure: Intracellular dynamics $u_{2j}(t)$ at two points in the scatter plot: Left: $D = 4$, $\sigma = 1/2$: wave-packet type-solution? or is it bad numerics? (hopefully not!) Right: $D = 2$, $\sigma = 1/6$: regular oscillations for second cell but with smaller amplitude.

Two-Cell Patterns: One Activated Cell III

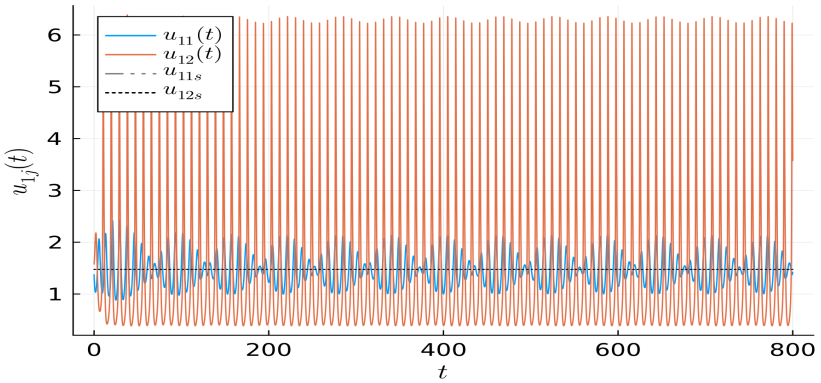

(a) u_{1j} fast algorithm

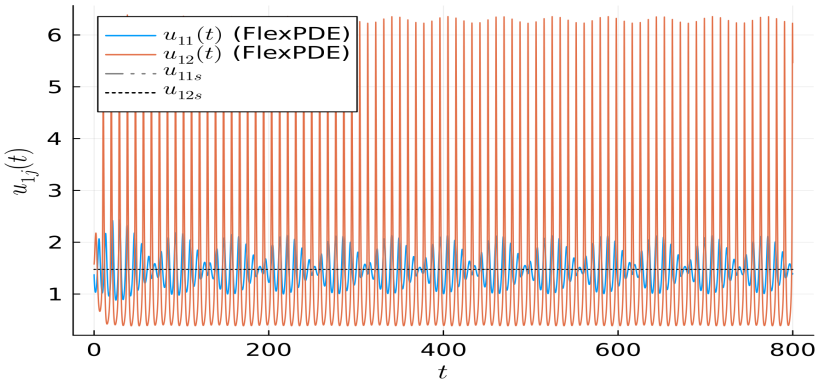

(b) u_{1j} FlexPDE

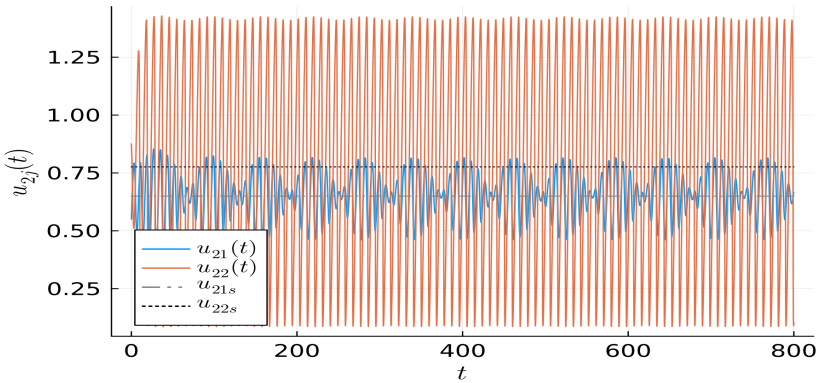

(c) u_{2j} fast algorithm

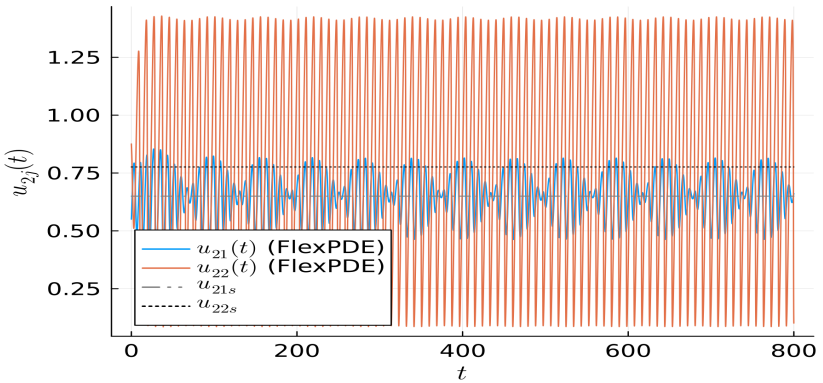

(d) u_{2j} FlexPDE

Figure: Parameters: $D = 3$, $\sigma = 1/2$. The IC was the anti-phase perturbation: $\boldsymbol{u}_1^{(0)} = (u_{11s}, u_{21s})^T + 0.01 \cdot (1, -1)^T$. Similar for $\boldsymbol{u}_2^{(0)}$. Fast algorithm reproduces the wave-packet oscillations of cell 2 over long time intervals.

Hexagonal Ring Pattern: One-Shell I

Fix $r_c = 2$. Ring cells identical. Center cell x_7 either "active" or "deactivated"

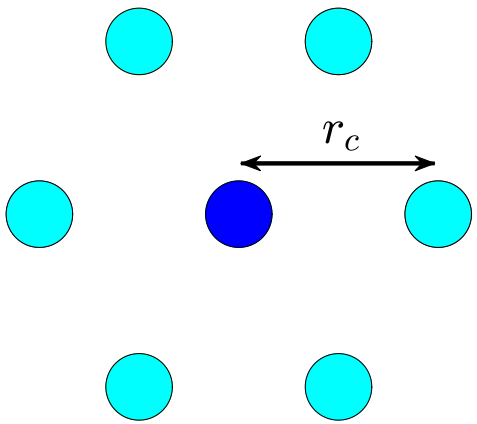

Case I: All cells identical with $d_{1r} = d_{17} = 0.4$, $d_{2r} = d_{27} = 0.2$ and $\alpha_r = \alpha_7 = 0.9$. Each cell would be in a quiescent state without any cell-cell coupling.

Case II: Identical ring cells have $d_{1r} = 0.8$, $d_{2r} = 0.2$ and $\alpha_r = 0.9$. Center cell is activated with $d_{17} = 0.4$, $d_{27} = 0.2$ and $\alpha_7 = 0.5$.

Case III: Same as Case II except that $d_{27} = 0.5$. Now the center cell is deactivated.

Hexagonal Ring Pattern: One-Shell II

Scatter plots in the $1/\sigma$ vs. D plane for Cases I, II, and III:

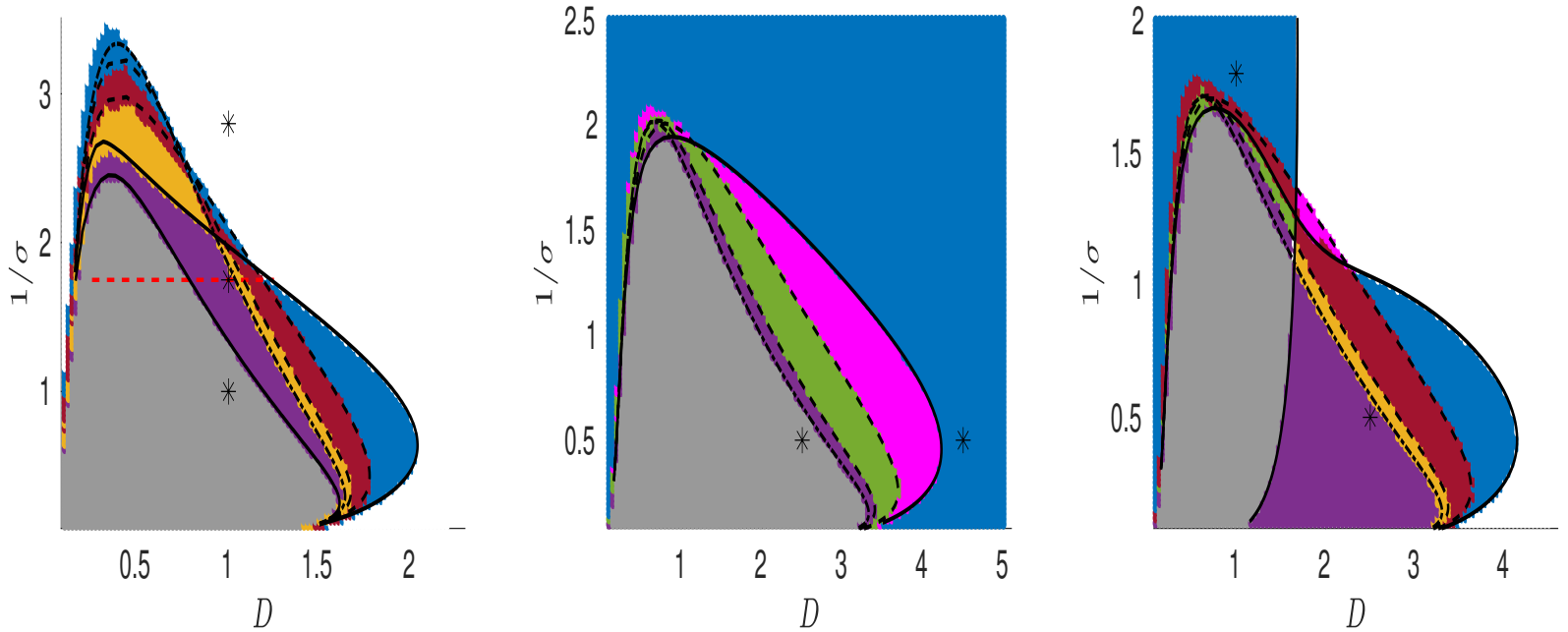

(a) I: identical cells (b) II: center active (c) III: center deactivated

Figure: $\mathcal{Z} = 0$ (white), $\mathcal{Z} = 2$ (blue), $\mathcal{Z} = 4$ (magenta), $\mathcal{Z} = 6$, $\mathcal{Z} = 8$ (green), $\mathcal{Z} = 10$ (orange), $\mathcal{Z} = 12$ (purple) and $\mathcal{Z} = 14$ (gray). The Kuramoto order parameter is computed on the red-dashed path for identical cell Case I.

Hexagonal Ring Pattern: Identical Cells

Kuramoto order parameter: Compute over $0 < t < 1500$ **with** $\Delta t = 0.005$**:**

$$Q(t) \equiv \frac{1}{N}\left|\sum_{j=1}^{N} e^{i\theta_j}\right|, \quad \text{where} \quad \theta_j \equiv \arctan\left(\frac{u_{2j}(t) - u_{2js}}{u_{1j}(t) - u_{1js}}\right) \in (0, 2\pi),$$

with u_{1js} and u_{2js} steady-states. Time-window: $t_{low} = 1300$ and $t_{up} = 1500$:

$$Q_{ave} = \frac{1}{t_{up} - t_{low}} \int_{t_{low}}^{t_{up}} Q(t)\, dt\,.$$

Left: Random IC (near SS). Right: Sign-Alternating IC (near SS). Magnitude 0.1

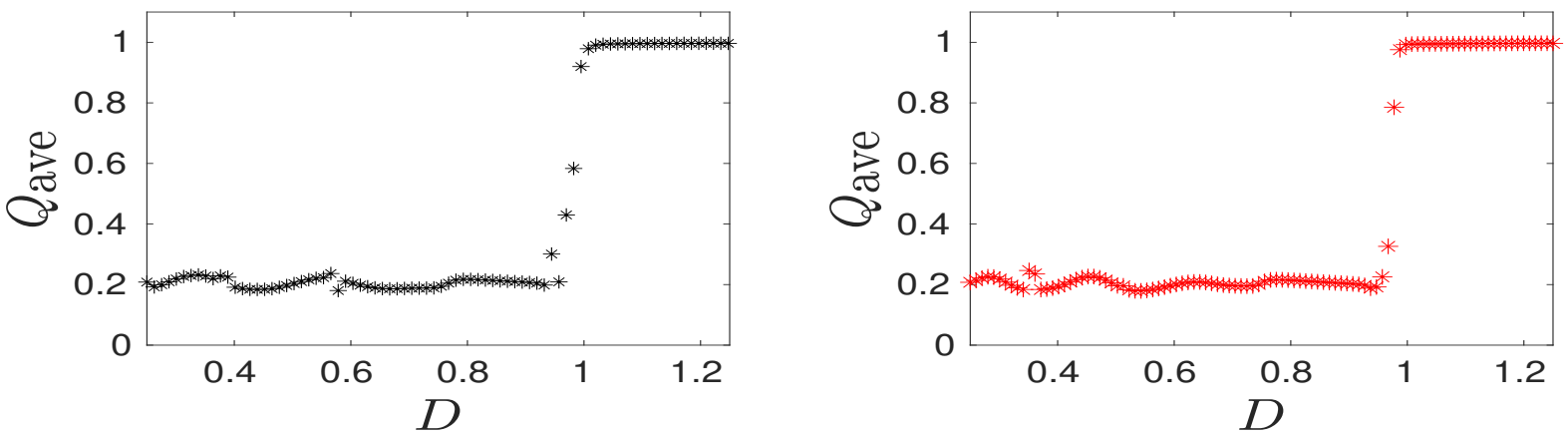

Figure: Q_{ave} vs. D for $\sigma = 4/7$ on $0.25 < D < 1.25$ along red dashed-path. A phase transition to phase coherence occurs when D is near unity.

Hexagonal Ring Pattern: Identical Cells

Top: $D = 0.75$: **Middle:** $D = 1$. **Right:** $D = 1.25$. Fast Algorithm: $u_{2j}(t)$.

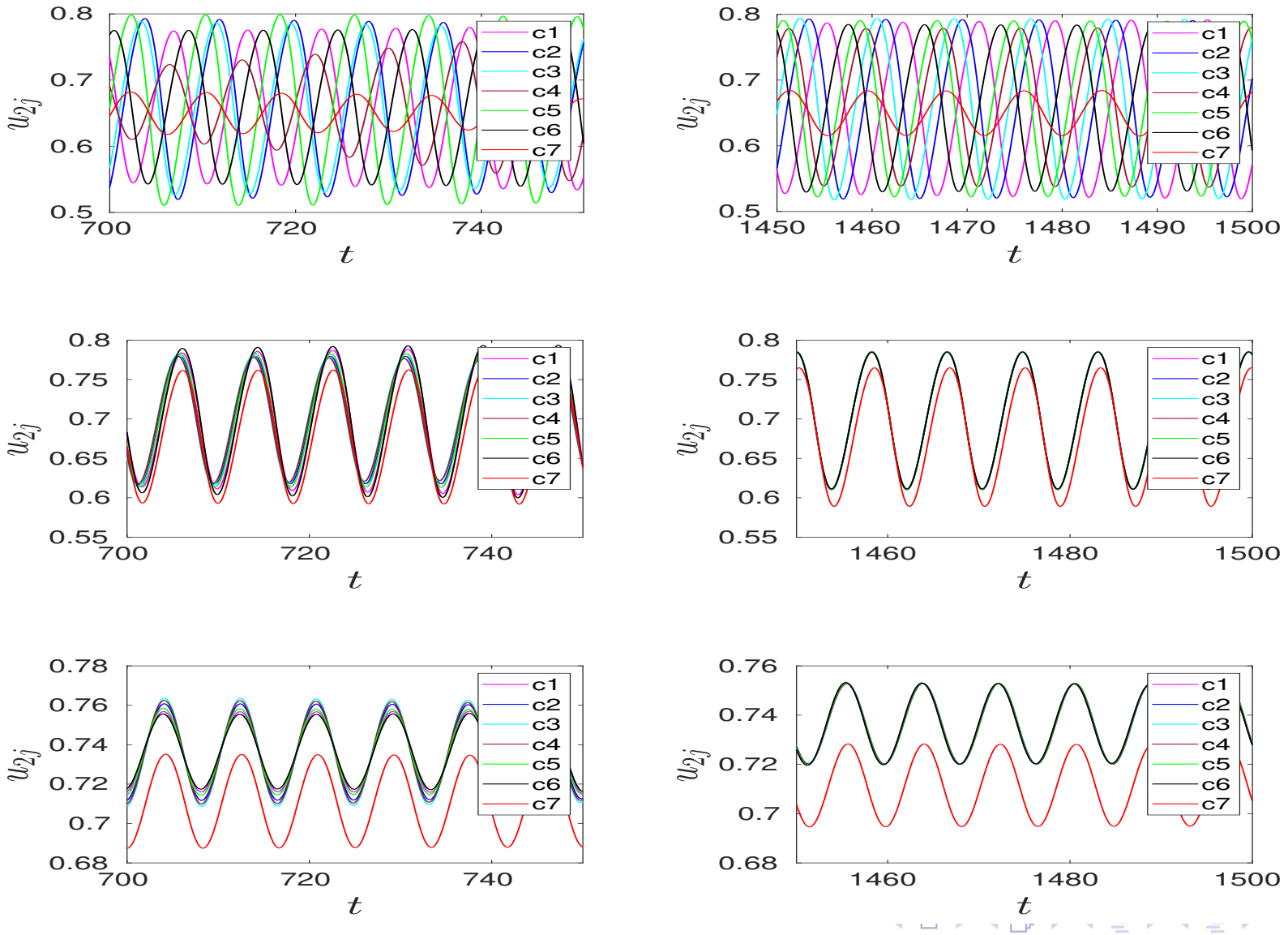

Hexagonal Ring Pattern: Non-Identical Cells

Case II: Center-Cell C7 is activated:

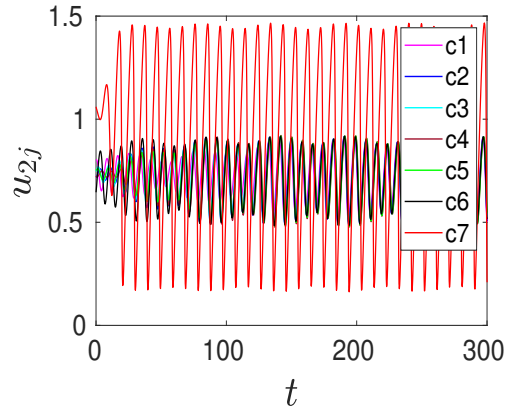

(a) $D = 2.5$, $\sigma = 2$

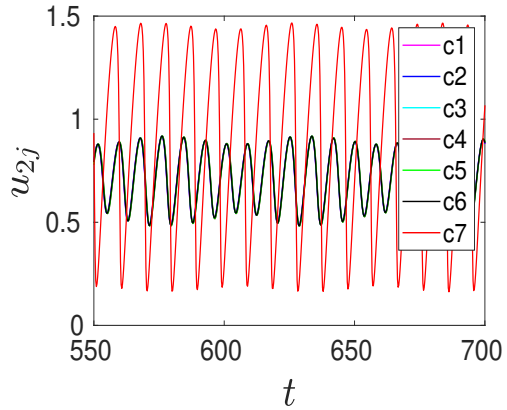

(b) $D = 2.5$, $\sigma = 2$

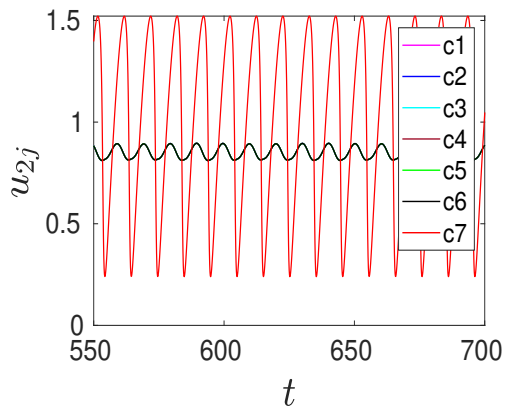

(c) $D = 4.5$, $\sigma = 2$.

Case III: Center-Cell C7 is now deactivated:

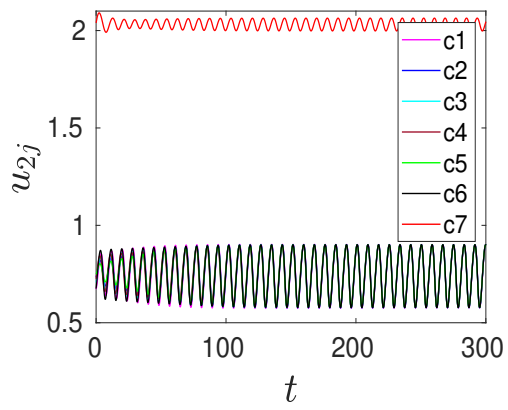

(a) $D = 2.5$, $\sigma = 2$

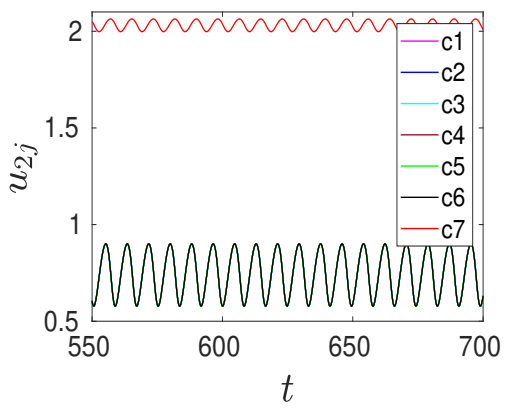

(b) $D = 2.5$, $\sigma = 2$

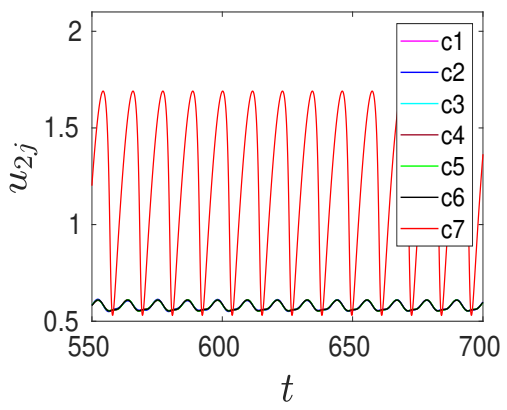

(c) $D = 1$, $\sigma = 5/9$

Centered Hexagonal Pattern: I

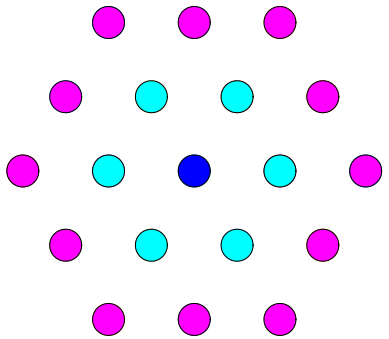

Figure: A centered hexagonal configuration of cells with two shells. Each shell has identical quiescent cells, while the center cell is "activated". Lattice generators: $\boldsymbol{L}_1 = \left(\left(\frac{4}{3}\right)^{1/4}, 0\right)^T$ and $\boldsymbol{L}_2 = \left(\frac{4}{3}\right)^{1/4}\left(\frac{1}{2}, \frac{\sqrt{3}}{2}\right)^T$, so that $|\boldsymbol{L}_1 \times \boldsymbol{L}_2| = 1$.

Experiment: For all 19 cells: $d_{1j} = 0.8$ (influx) and $d_{2j} = 0.2$. The center cell has $\alpha_1 = 0.5$, and so is activated. Inner inner and outer shells: $\alpha_j = 0.7$ and $\alpha_j = 0.8$. These cells are all quiescent when uncoupled from bulk.

- For $\sigma = 1$ and $D = 0.3$: $Q_{ave} = 0.237$: Rather little phase coherence.
- For $\sigma = 1$ and $D = 0.7$: $Q_{ave} = 0.975$: Strong phase coherence.

Key Conclusion: One single "active" cell can lead to strong phase coherence for the ENTIRE cell population as D increases past a threshold.

Centered Hexagonal Pattern: II

Top: $D = 0.3$. **Middle:** $D = 0.5$. **Bottom:** $D = 0.7$. **Fast Algorithm:** $u_{2j}(t)$.

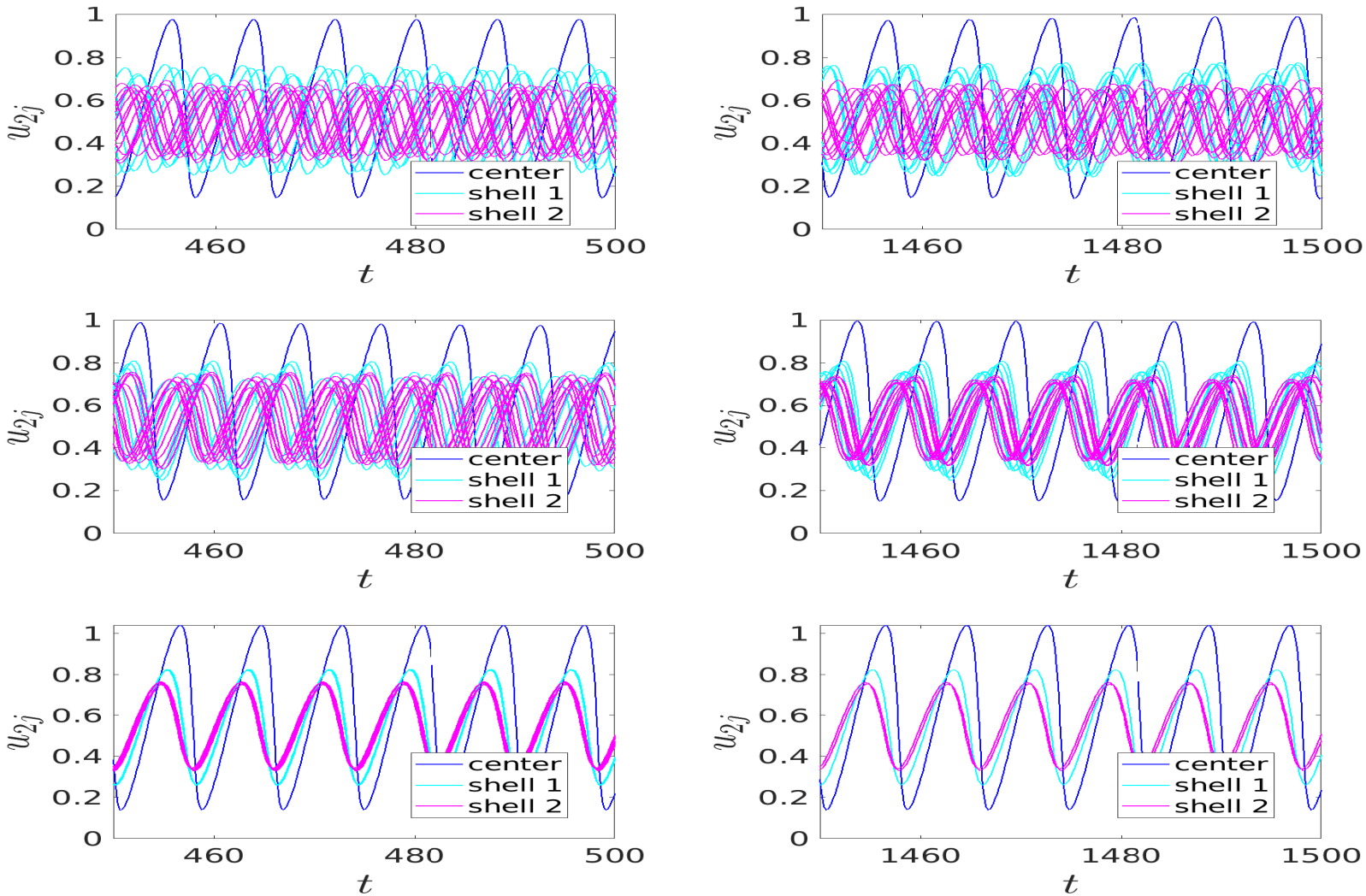

Discussion

Ref: M. Pelz, M. J. Ward, *Synchronized Memory-Dependent Intracellular Oscillations for a Cell-Bulk ODE-PDE Model in* $\mathbb{R}^2$, SIADS **24**2, (2025), (60 pages).

Summary: The new memory-dependent integrodifferential system replaces the usual Kuramoto ODE-paradigm for modeling situations where the intracellular dynamics for a collection of cells is coupled through a 2-D time-dependent bulk-diffusion field.

End-Game: Fast-algorithm allows exploration of synchronization for large N large with Kuramoto order parameter; identify possible chimera states and pattern-formation aspects such as discrete spiral waves and target patterns induced by bulk-mediated coupling.

Hybrid Analytic-Numerical Approach: Classical analytical applied math techniques (singular perturbations, transforms, special functions, complex analysis) used together with some modern innovative numerical approaches (sum-of-exponential method, marching schemes, nonlinear matrix eigenvalue problems).

Viable Extensions: Cell-bulk with two-bulk species, 3-D cell-bulk, include drift fields, finite domains. Next step: explore specific applications in math bio (glycolysis) and chemical physics (microemulsions).

Topic II: Binding-Mediated Diffusion

Classical Turing: Let the activator u and inhibitor v satisfy

$$u_t = D_u u_{xx} + f(u,v)\,, \quad v_t = D_v v_{xx} + g(u,v)\,; \quad u_x = v_x = 0\,, \ \ x = 0, L\,.$$

Turing Analysis: Suppose that the base state (u_e, v_e), where $f(u_e, v_e) = g(u_e, v_e) = 0$, is linearly stable when $D_u = D_v = 0$, i.e. $\mathrm{Tr}(J_e) < 0$ and $\det(J_e) > 0$, where J_e is Jacobian of the kinetics, with $f_u^e > 0$ and $g_v^e < 0$. A necessary condition for its instability with diffusion is

$$\frac{D_v}{D_u} f_u^e + g_v^e > 2\sqrt{\frac{D_v}{D_u}\det(J_e)}\,, \qquad \text{(The DDR condition)}\,.$$

Challenge: The DDR condition for onset of (symmetry-breaking) spatial patterns from the base state usually needs D_v/D_u to be significantly larger than unity. However, in many biological and chemical systems "freely" diffusing morphogens (small molecules) have comparable diffusivities.

Key Question: How to obtain symmetry-breaking without the need for a possibly unrealistically large differential diffusivity ratio condition?

Overcoming the DDR condition

- Fine-tuning kinetics to near neutrally stable spatially uniform states (J. Pearson, JChemPhys **90** (1989)). (Not a robust mechanism).
- Adding immobile species to make a "2+1" component system, where added species is non-diffusing (V. Klika et al., BMB **74**(2012); K. Korvasova et al., J. Theor. Bio. **367**, (2015); (Can lead to spatial discontinuities).
- Random RD sytems with many components can partially overcome the DDR requirement (Haas and Goldstein, Phys. Rev. Lett **126**, (2021)). (Large computational study, hard to analyze).

Other models have ligand binding effects being a key mechanism for pattern formation:

- **Bulk-membrane or bilayer RD systems:** RD processes inside a domain are coupled to RD processes on the surface (Levine and Rappel, Phys. Rev. E. **72** (2005); Madzvamuse et al. Proc. Roy. Soc. A, **471**, (2015); Paquin-Lefebvre et al., SIADS **18**(2019); Krause et al. BMB, **82**(2020)).
- **Agent-Based Models:** Discretized Diffusion in 2-D and Localized Reactions: Rauch and Millonas, J.Theo. Bio., **226**(2004). "In the mechanism we propose, reactions occur within cells. Signal transduction leads to the production of messenger molecules, which diffuse between cells at approximately equal rates, coupling the reactions occurring in different cells."

Motivation: Cell-Bulk model with 2 Bulk Species

Binding-Mediated Diffusion in Biology

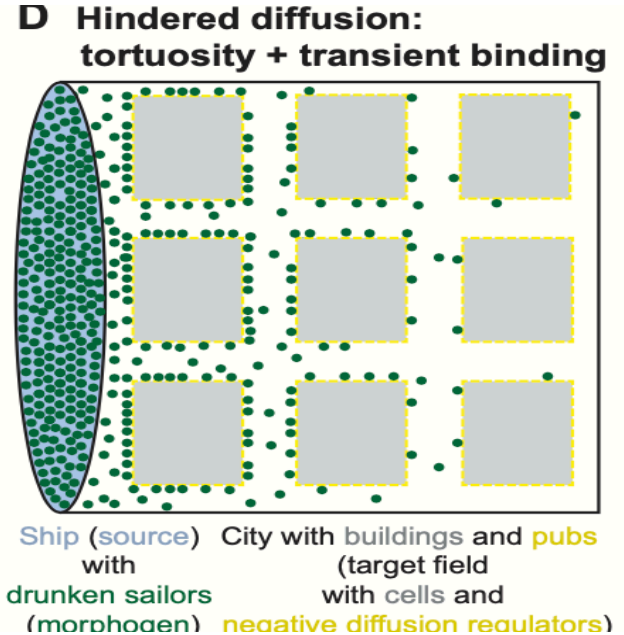

- Many postulated mechanisms for morphogen transport: **Ref:** P. Muller et al., *Morphogen Transport*, Development **140**, (2013). ("Drunken sailor model").
- Hindered-diffusion or binding-mediated diffusion is a key model for tissues: **Ref:** Stapornwongkul and Vincent, Nat. Rev. Genetics, **22**, 2021.
- Conditions for the emergence of asymmetry is important in embryogenesis: **Ref:** Sozen et al., Development, **474**, (2021).

"Morphogens diffuse freely in the extracellular space, but tissue geometry and transient binding interactions affect spreading. Therefore, one can distinguish between free (or local) and effective diffusion rates. Whereas free diffusivity depends on the molecule's size, effective diffusivity takes into account the effect of morphogen binding and unbinding to receptors on cell surfaces and in the extracellular matrix." **Ref:** K. Stapornwongkul, J. Briscoe *Development*, (2022)

Motivation: Cell-Bulk with 2 Bulk Species

Binding-mediated diffusion: Freely diffusing species can bind at different rates to ligands on the compartment boundaries. **Our Conjecture:** This introduces "effective" diffusion coefficients whose ratio may be large enough for "symmetry-breaking".

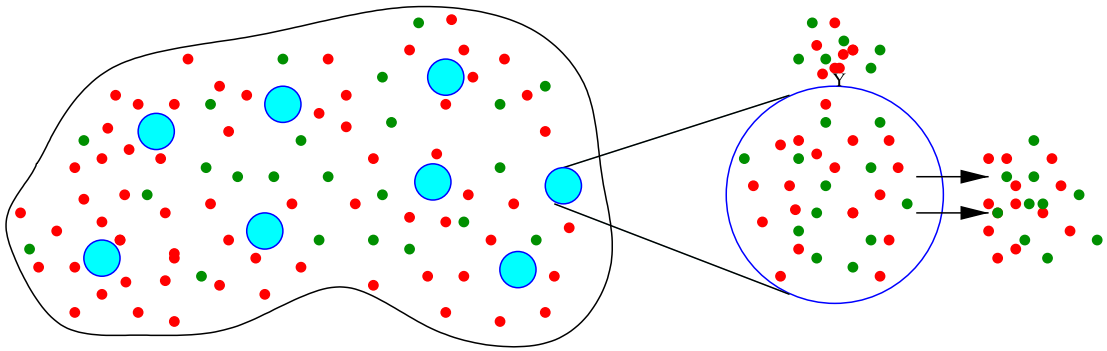

Key: Binding rates modeled by Robin BC on the cell boundaries.

Specific Goal: Formulate and analyze a 2D bulk cell model with identical activator-inhibitor kinetics restricted to "cells". Assume identical bulk parameters.

Key Question: Is the ratio of inhibitor to activator membrane binding rates a key bifurcation parameter allowing for "symmetry-breaking"?

Ref: M. Pelz, MJW, *Symmetry-Breaking Bifurcations for Compartmental RD systems in 2-D*, Frontiers in Applied Math, **9**, (2023).

Ref: M. Pelz, MJW, Phil. Trans. Roy. Soc. **A381**, (2023). (1-D theory).

PDE-ODE Model in 2-D: Dimensionless Formulation

For $\Omega \in \mathbb{R}^2$, the N reaction compartments Ω_j are disks of a common radius $\varepsilon \ll 1$: $\Omega_j = \{\boldsymbol{x} \mid |\boldsymbol{x} - \boldsymbol{x}_j| \leq \varepsilon\}$. Assume disks are well-separated $|\boldsymbol{x}_i - \boldsymbol{x}_j| = \mathcal{O}(1)$ for $i \neq j$.

In the bulk region, the bulk fields U, V satisfy

$$U_t = D_u \Delta U - \sigma_u U, \qquad V_t = D_v \Delta V - \sigma_v V\,, \quad \boldsymbol{x} \in \Omega \setminus \cup_{j=1}^{N} \Omega_j\,,$$
$$\varepsilon D_u \partial_n U = d_{1,j} U - d_{2,j} \xi_j\,, \quad \varepsilon D_v \partial_n V = b_{1,j} V - b_{2,j} \eta_j, \quad \boldsymbol{x} \in \partial\Omega_j, \quad \forall j\,,$$
$$\partial_n U = 0, \quad \partial_n V = 0, \quad \boldsymbol{x} \in \partial\Omega\,,$$

and are coupled to intracellular reaction kinetics $\mathrm{F}_j \in \mathbb{R}^2$ for $j = 1, \ldots, N$ by

$$\frac{d\boldsymbol{u}_j}{dt} = \boldsymbol{F}_j(\boldsymbol{u}_j) + \boldsymbol{e}_1 \int_{\partial\Omega_j} (d_{1,j} U - d_{2,j} \eta_j)\, dS + \boldsymbol{e}_2 \int_{\partial\Omega_j} (b_{1,j} V - b_{2,j} \eta_j)\, dS\,,$$

where $\boldsymbol{u}_j = (\mu_j, \eta_j)^T$, $\boldsymbol{e}_1 = (1,0)^T$ and $\boldsymbol{e}_2 = (0,1)^T$.

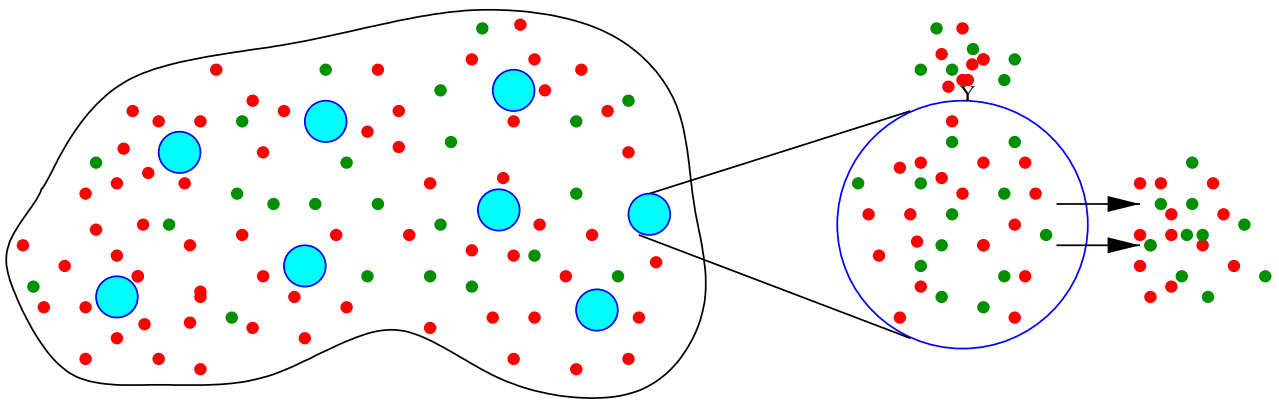

Theoretical Framework for Analysis

- Singular perturbation analysis for $\varepsilon \to 0$ to construct steady-states and derive linear stability problem. No spatially uniform steady-state in general.
- Global steady-states found from a nonlinear algebraic system (NAS) in terms of the reduced-wave Green's function G for Ω.
- Linearized stability: Eigenvalue problem for point spectra involves root finding on a nonlinear matrix eigenvalue problem (GCEP) (challenging in general!).

Question: Is "Symmetry-Breaking" controlled by a ratio of membrane binding rates?

Simplest Configurations: Ring type: cells equidistantly spaced on a ring concentric within a disk. $\exists$ a symmetric steady-state solution (SSS) when $\mathsf{F}_j = \mathsf{F}\ \forall j$. Can stable asymmetric-equilibria bifurcate from the SSS by varying the binding rate ratio?

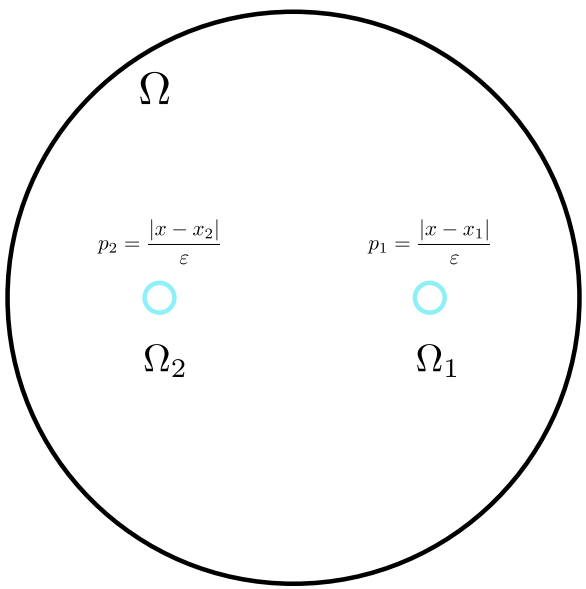

$$m = 2$$
$$d_v = \rho\, d_u$$
$$\rho > 1, d_u > 0$$
$$D_u = D_v$$

Key: circulant matrix structure for the NAS and the GCEP allow for a much simpler analysis.

GM Kinetics: A Two-Cell Ring Pattern

Consider GM reaction kinetics $\mathrm{F} \equiv \left(\mu^2/\eta, \mu^2\right)^T$ common to the two cells.

Let Ω be unit disk. Bulk parameters: common diffusivites $D_u = D_v = 5$ and $\sigma_u = \sigma_v = 0.6$. Cell radius: $\varepsilon = 0.03 \ll 1$. Ring radius: $r = 0.5$. Membrane binding rates: $d_{1,j} = d_{2,j} \equiv d_u = 0.09$ and $b_{1,j} = b_{2,j} \equiv d_v$.

Bifurcation Parameter: $\rho \equiv d_v/d_u$. What is effect of varying ring radius r?

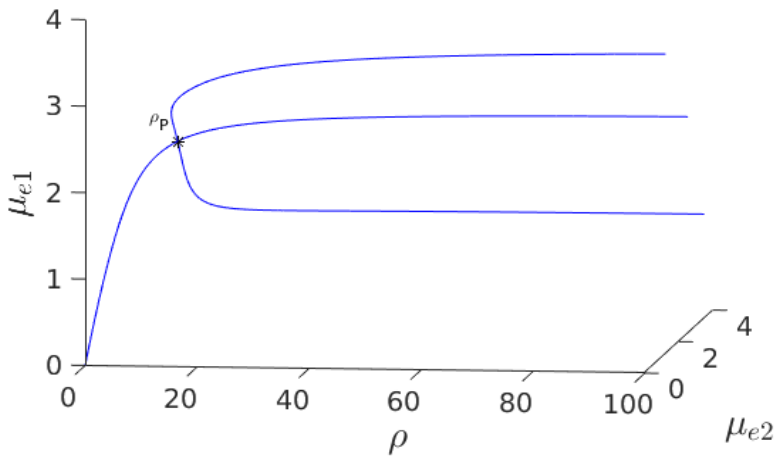

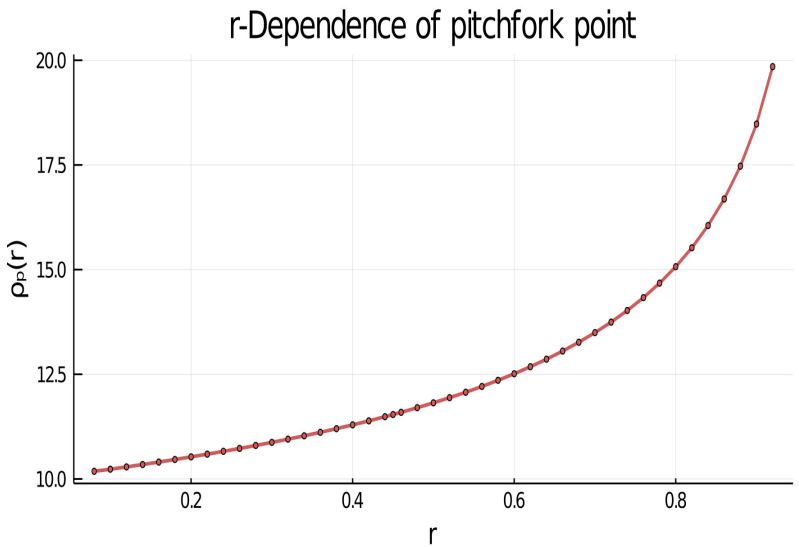

Linearly stable asymmetric steady-states emerge at a supercritical pitchfork point ρ_p along the SSS branch. Right: ρ_p increases rapidly as the ring radius r (i.e. distance) between the cells increases.

FlexPDE: Confirmation of Theory

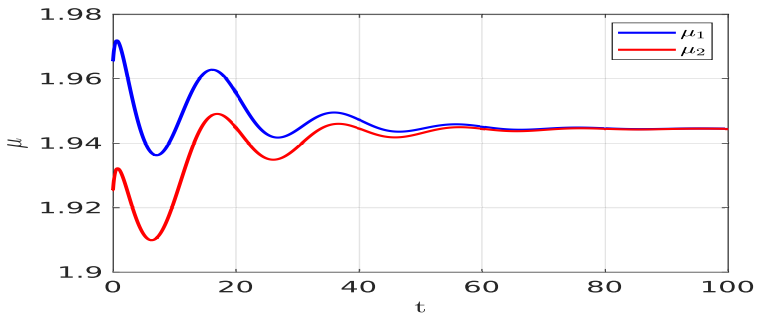

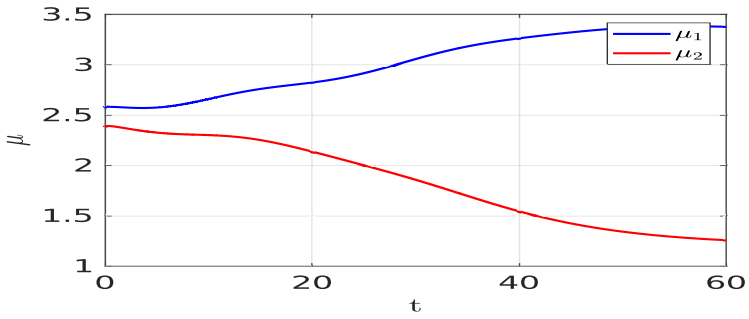

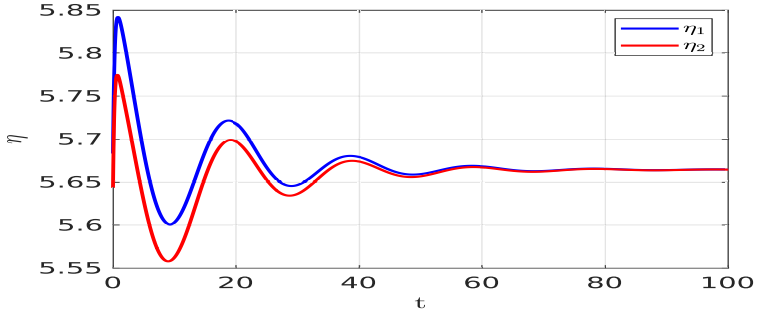

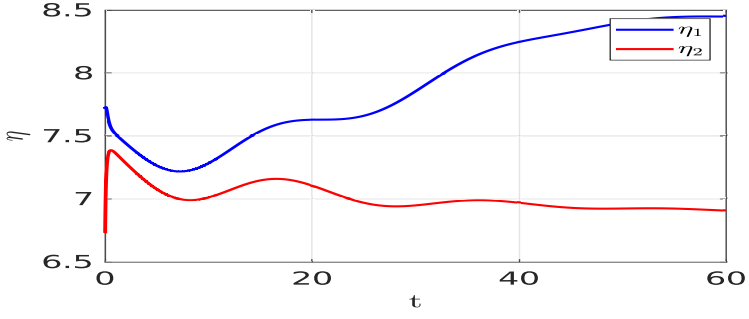

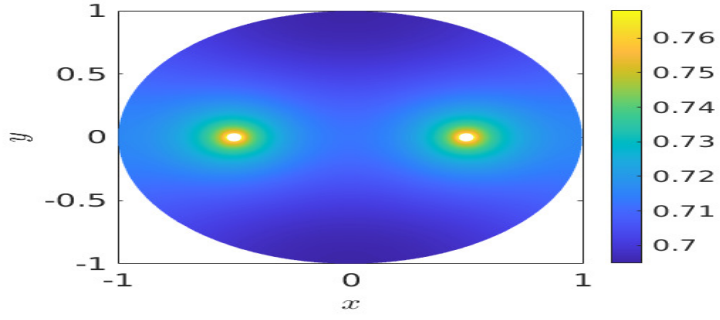

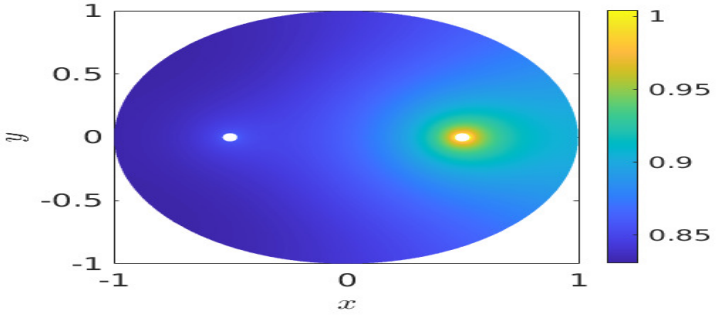

FlexPDE simulations:: Left: convergence to the SSS for $\rho = 5 < \rho_p$. Right: convergence to a stable asymmetric steady-state for $\rho = 15 > \rho_p$.

Hysteresis for GM kinetics: Varying d_u.

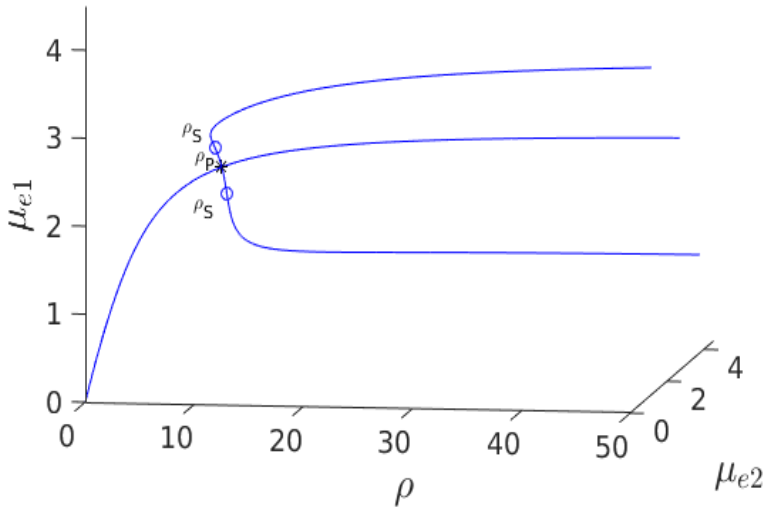

(a) $d_u = 0.08$

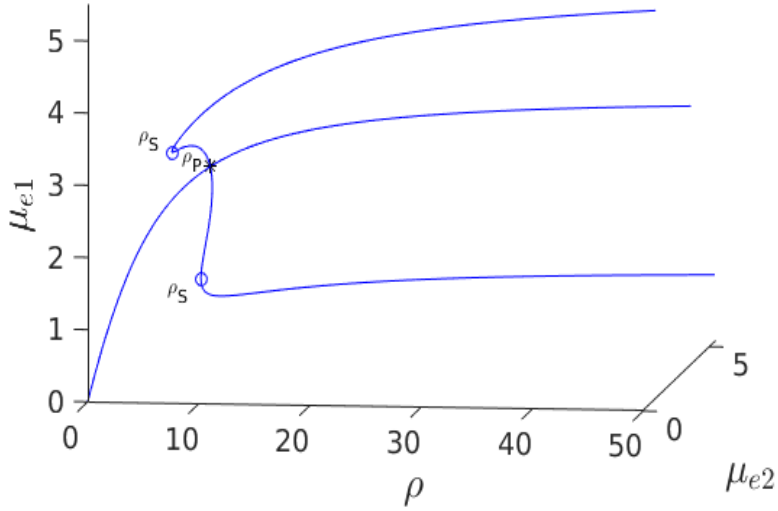

(b) $d_u = 0.05$

3-D Bifurcation diagram for symmetric and asymmetric steady-states of a two-cell ring pattern with ring radius $r = 0.5$ with GM kinetics. Hysteresis is observed: a subcritical pitchfork bifurcation occurs from the SSS branch at $\rho = \rho_p$ with emerging unstable asymmetric steady-states (ASS) regaining stability at a secondary fold point ρ_s. Extent of hysteresis increases when d_u decreases. Parameters: $D_u = D_v = 5$, $\sigma_u = \sigma_v = 0.6$, $\varepsilon = 0.03$, and $r = 0.5$.

Confirmation of Hysteresis for GM with FlexPDE

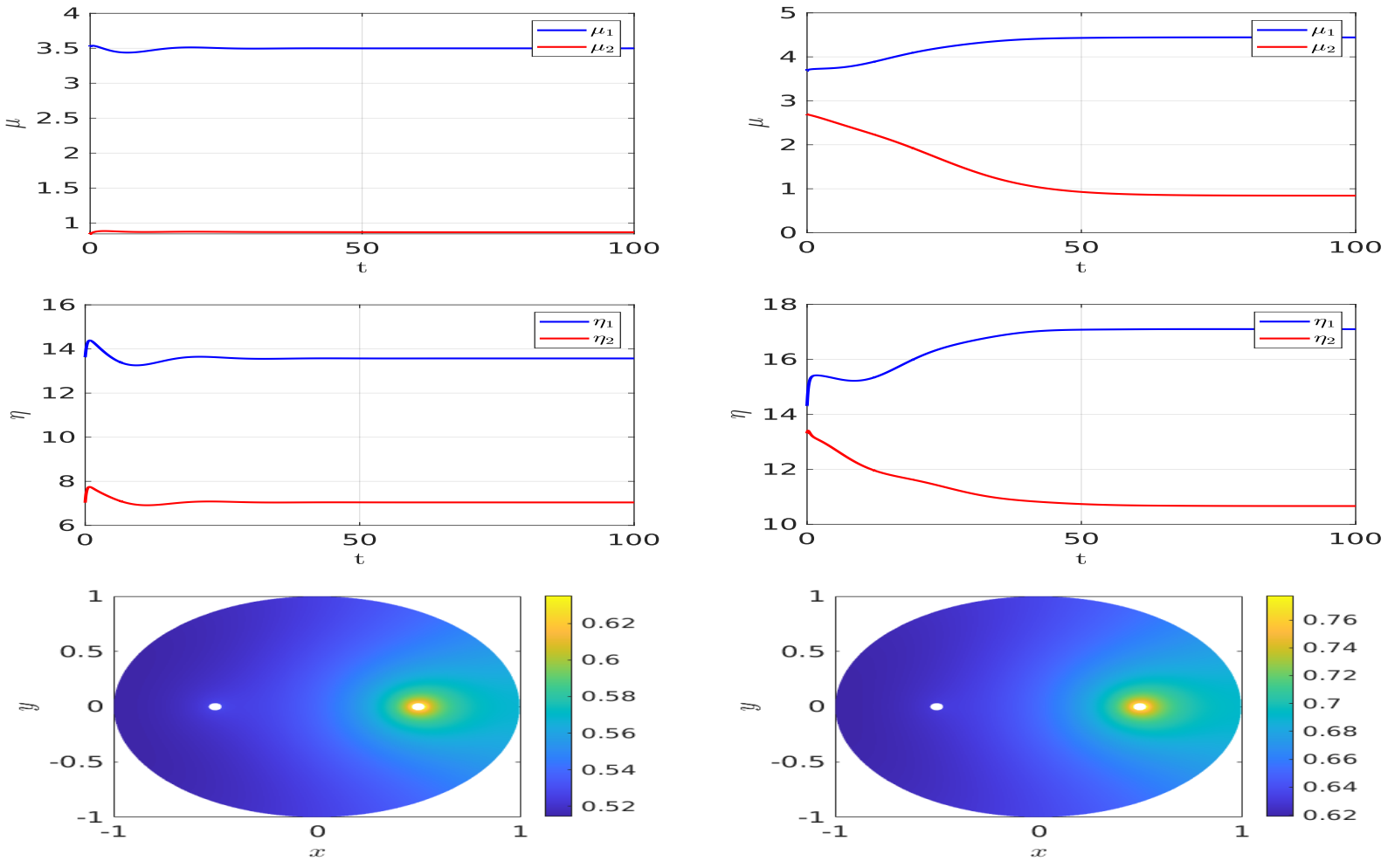

FlexPDE results $d_u = 0.08$: Left: convergence to asymmetric SS for nearby IC when $\rho = 7.2$ is in hysteresis band $\rho_s \approx 6.28 < \rho < \rho_p \approx 7.71$. Right: convergence to asymmetric SS for $\rho = 15 > \rho_p$. IC is small anti-phase perturbation of the SSS.

Hysteresis for GM: Varying d_u or D_v/D_u

Varying d_u: $D_v = D_u = 5$. Transition from sub- to super-criticality.

d_u	0.05	0.06	0.07	0.08	0.09	0.1	0.11	0.12	0.13	0.135
ρ_p	7.71	7.67	11.42	8.62	9.79	11.82	15.65	24.82	70.62	> 1000 or $\nexists$
μ_e	2.78	2.55	3.21	2.28	2.20	2.14	2.10	2.06	2.04	
ρ_s	6.28	6.93	6.83	8.60	-	-	-	-	-	-
μ_{e1}	3.27	3.09	3.46	2.56	-	-	-	-	-	-
μ_{e2}	1.12	1.35	0.88	1.93	-	-	-	-	-	-

Pitchfork point ρ_p for SSS and fold points ρ_s for ASS vs. d_u. Supercritical pitchfork emerges at $d_u = 0.85$. Other parameters: $\sigma_u = \sigma_v = 0.6, \varepsilon = 0.03, r = 0.5$.

Varying D_v: $d_u = 0.8$ and $D_u = 5$ (same other parameters).

D_v/D_u	0.37	0.38	0.4	0.6	0.8	1	3	5	8
ρ_p	> 1000 or $\nexists$	198.0	72.6	14.3	10.1	8.62	6.13	5.79	5.61
μ_e		2.44	2.43	2.34	2.30	2.28	2.22	2.20	2.19
ρ_s		188.6	71.3	14.2	10.0	8.60	6.12	5.78	5.60
μ_{e1}		2.74	2.72	2.63	2.59	2.56	2.49	2.48	2.47
μ_{e2}		2.06	2.05	1.98	1.95	1.93	1.88	1.87	1.86

Note: Hysteresis still occurs when $d_u = 0.08$ as D_v/D_u is increased. Pitchfork from SSS occurs EVEN for some range of $D_v/D_u < 1$! (when inhibitor is slow diffuser)

Topic II: Discussion I

Framework: Compartmental RD models in 2-D provide a conceptual framework for modeling binding-mediated diffusive transport with two bulk species.

2D Extension: Analyze periodic cell arrangements in $\mathbb{R}^2$. Symmetry-breaking bifurcations for a spatially periodic steady-state (the "SSS" pattern) of small cells centered at lattice points of a 2-D Bravais lattice (e.g Hexagonal lattice), as controlled by membrane binding rate ratio.

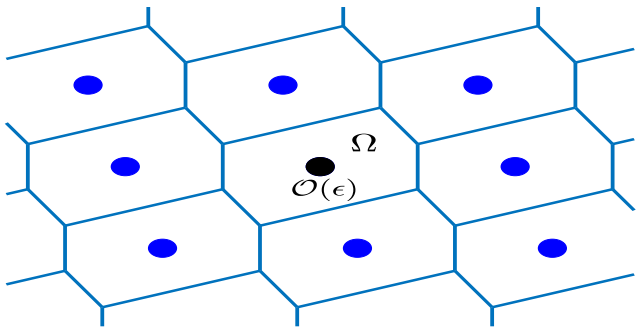

- **Technical Challenge:** "Bifurcation" from edge of continuous spectrum.
- Key for analysis: An explicit Floquet-Bloch reduced-wave G-function (Belykin).
- Which "anti-phase" Floquet-Bloch mode in Brilloiun zone leads to symmetry-breaking?
- Develop a weakly nonlinear theory to predict sub- or super-critical (in progress).

Topic II: Discussion II

Take-away: Binding ratio of the two species on the compartments can control the emergence of *symmetry-breaking* bifurcations of a SSS ($\rightarrow$ stable asymmetric equilibria) even when bulk diffusivities are equal. Robust mechanism for generating stable asymmetric steady-states. Similar results to GM for Rauch-Millonas or FitzHugh-Nagumo intracellular kinetics, but now also possibility of Hopf bifurcations.

Biological Limitation: In 2-D, asymptotic analysis needs small compartment radii and spatially segregated compartments (not applicable to tissues). Can we instead consider asymptotic limit of binding-mediated diffusion on checkerboard patterns with $\mathcal{O}(1)$ cells or with thin "roads"?

Need Different Asymptotics and More Numerics:

- Homogenization approach likely useful.
- Thin channel asymptotics: reduction of PDE to a network model?
- Numerics needed for steady-state and stability problem in Wigner-Seitz cell. (open)